THE ROLE OF TGF-β ACTIVATED KINASE (TAK1) IN RETINAL DEVELOPMENT AND INFLAMMATION

by

Casandra Carrillo

A Thesis

Submitted to the Faculty of Purdue University

In Partial Fulfillment of the Requirements for the degree of

Master of Science

Department of Biology at IUPUI

Indianapolis, Indiana

August 2021

THE PURDUE UNIVERSITY GRADUATE SCHOOL

STATEMENT OF COMMITTEE APPROVAL

Dr. Teri Belecky-Adams, Chair

Department of Biology

Dr. A.J. Baucum

Department of Biology

Dr. Nicolas Berbari

Department of Biology

Approved by:

Dr. Theodore Cummins

“The greatest teacher, failure is” -Yoda

This thesis is dedicated to my parents and my fiancé, for being constant and unwavering in their support.

ACKNOWLEDGMENTS

This thesis project would not have been possible without the guidance, encouragement, and support of my mentor Dr. Belecky-Adams. I am fortunate to have such a kind and inspiring mentor. I have learned more than I thought possible. I am grateful and look forward to continuing my PhD in the Belecky-Adams lab.

I would like to thank the members of my committee, Dr. AJ Baucum and Dr. Nicolas Berbari, for their support throughout my thesis project. Their thought-provoking questions helped aid my critical thinking of this thesis project and its execution.

I would also like to thank my parents; their constant support and encouragement has made it possible for me to pursue my dreams of becoming a scientist.

Lastly, I would like to thank my partner, Brian Wyatt. Words cannot express how grateful I am for the unwavering support, patience, and encouragement he has given me throughout stressful deadlines, failed experiments, and finalizing this thesis project during a global pandemic.

TABLE OF CONTENTS

LIST OF TABLES

LIST OF FIGURES

LIST OF ABBREVIATIONS

AGE	Advanced Glycation End Products
AKITA or AK	InsAkita
AP-2alpha	Activating Enhancer Binding Protein 2 Alpha
ATG5	Autophagy Related 5
BBB	Blood Brain Barrier
BCA	Bicinchoninic Acid
bHLH	Basic Helix-Loop-Helix
BMP	Bone Morphogenic Protein
BOD	Biochemical Oxygen Demand
BRB	Blood Retinal Barrier
BRN3a	Brain-Specific Homeobox/POU Domain Protein 3A
c-Myc	Cellular Myelocytomatosis
CC3	Cleaved Caspase-3
CDK	Cyclin-Dependent Kinase
Chx10	CEH10 Homeodomain-Containing Homolog
CIP	CDK Interacting Protein
CNS	Central Nervous System
CO2	Carbon Dioxide
Damps	Damage-associated molecular pattern
DB or db/db	LeprDB
DMEM	Dulbecco's Modified Eagle Medium
DR	Diabetic Retinopathy
EDTA	Ethylenediaminetetraacetic Acid
ERK	Extracellular-Signal-Regulated Kinase
F12	Ham's F-12 Nutrient Mixture
FBS	Fetal Bovine Serum
GABA	Gamma Aminobutyric Acid

GCL	Ganglion Cell Layer
IACUC	Institutional Animal Care and Use Committee
iBRB	Inner Blood Retinal Barrier
ICC	Immunocytochemistry
IFNγ	Interferon Gamma
IkB	IκB Kinase
IKK	Inhibitor of NF-kB Kina
ILM	Inner Limiting Membrane
INL	Inner Nuclear Layer
Islet1	Insulin Gene Enhancer Protein ISL-1
JNK	c-Jun N-Terminal Kinase
KIP	CDK Kinase Inhibitory Protein
LIM ½	LIM Kinase 1 and LIM Kinase 2
LPS	Lipopolysaccharide
MAP3K	MAP Kinase Kinase Kinase
MAP3K7/TAK1	MAP Kinase Kinase Kinase 7
MAPK	Mitogen Activated Protein Kinase
MeOH	Methanol
MHC	Major Histocompatibility Complex
NAPA-73	Neurofilamaent-Associated Protein, 73 kDa
NBL	Neural Blast Layer
NFkB	Nuclear Factor Kappa-Light-Chain-Enhancer of Activated B Cells
NFL	Neural Fiber Layer
NG2	Neural/Glial Antigen 2
NOS	Nitric Oxide Synthase
NVU	Neurovascular Unit
oBRB	Outer Blood Retinal Barrier
OCT	Optimal Cutting Temperature Compound
OLM	Outer Limiting Membrane

ONL	Outer Nuclear Layer
OPL	Outer Plexiform Layer
p38	p38 Mitogen-Activated Protein Kinase
PAP	Peroxidase-Anti-Preoxidase
PAMPs	Pathogen-associated molecular pattern
PBS	Phosphate Buffered Saline
PBST	Phosphate Buffered Saline with Triton X-100
PDGF	Platelet-Derived Growth Factor
PDGF-BB	Platelet-Derived Growth Factor Homodimer BB
PDGFRβ	Platelet-Derived Growth Factor Receptor β
PDR	Proliferatice Diabetic Retinopathy
PERK	Pancreatic endoplasmic reticulum kinase
PFA	Paraformaldehyde
pH3	Phospho-Histone 3
pJNK	Phospho c-Jun
PKC	Protein Kinase C
pPDGFRβ	Phosphorylated PDGFRβ
RIPK ½	Receptor- Interacting Protein Kinase 1 & 2
SAC	Sacrifice
RNA	Ribonucleic Acid
ROS	Reactive Oxygen Species
RPC	Retinal Precursor Cell
RPE	Retinal Pigmented Epithelium
RT	Room Temperature
SHH	Sonic Hedgehog Signaling Molecule
Sox2	SRY (sex determining region Y)-box 2
STZ	Streptozotocin
TAB1	TAK1-Binding Protein 1
TGF- β	Tumor Growth Factor Beta

TLR	Toll-like Receptor
TNF	Tumor Necrosis Factor
TNFα	Tumor Necrosis Factor Alpha
TNT Buffer	Tween 20 Buffer
TSA	Tyramide Signal Amplification
VEGF	Vascular Endothelial Growth Factor
WT	Wild Type or C57BL/6

ABSTRACT

Carrillo, Casandra, M.S. Purdue University, August 2021. The Role of TGF- β Activated Kinase (TAK1) in Retinal Development and Inflammation. Major Professor: Teri Belecky-Adams.

Transforming growth factor β-activated kinase 1 (TAK1), a hub kinase at the convergence of multiple signaling pathways, is critical to the development of the central nervous system and has been found to play a role in cell death and apoptosis. TAK1 may have the potential to elucidate mechanisms of cell cycle and neurodegeneration. The Belecky-Adams laboratory has aimed to study TAK1 and its potential roles in cell cycle by studying its role in chick retinal development as well as its possible implication in the progression of diabetic retinopathy (DR). Chapter 3 includes studies that explore TAK1 in a study in chick retinal development and TAK1 in in vitro studies in retinal microglia. Using the embryonic chick, immunohistochemistry for the activated form of TAK1 (pTAK1) showed localization of pTAK1 in differentiated and progenitor cells of the retina. Using an inhibitor or TAK1 activite, (5Z)-7-Oxozeaenol, in chick eye development showed an increase in progenitor cells and a decrease in differentiated cells. This study in chick suggests TAK1 may be a critical player in the regulation of the cell cycle during retinal development. Results from experimentation in chick led to studying the potential role of TAK1 in inflammation and neurodegeneration. TAK1 has previously been implicated in cell death and apoptosis suggesting that TAK1 may be a critical player in inflammatory pathways. TAK1 has been implicated in the regulation of inflammatory factors in different parts of the CNS but has not yet been studied specifically in retina or in specific retinal cells. Chapter 2 includes studies from the Belecky-Adams laboratory of in vitro work with retinal microglia. Retinal microglia were treated with activators and the translocation to the nucleus of a downstream factor of TAK1 was determined: NF-kB. Treatment of retinal microglia in the presence of activators with TAKinib, an inhibitor of TAK1 activation, revealed that TAK1 inhibition reduces the activation of downstream NF-kB. Together this data suggests that TAK1 may be implicated in various systems of the body and further studies on its mechanisms may help elucidate potential therapeutic roles of the kinase.

CHAPTER 1. INTRODUCTION

The neural retina is a highly organized tissue located in the back of the eye. It is composed of neurons and glia, similar to the cell types that populate the central nervous system (CNS). The retina is an extension of the CNS and is responsible for taking in light and transducing it into signal that it then passes on to various parts of the brain. Cells within the retina undergo similar processes of signaling in development as well as in response to damage or inflammation to those in the rest of the CNS. The retina is a highly regulated tissue, containing the blood retinal barrier (BRB) which is formed by tight junctions that serve as a physiological barrier that regulates the movement of ions, proteins, and water in and out of the retina. This is like the blood brain barrier (BBB) in the brain that separates the circulation of blood from the neurons of the brain, protecting against neurotoxins and also serving as an ion transporter. Due to these similarities, the retina has long been used as a tool to study the CNS. Recent studies have implicated mitogen activated protein kinases (MAPKs) as possible key regulators within the retina during development. MAPK has also been implicated in disease states, inflammation, and cell death. The studies here aim to show that TGF-ß activated kinase 1 (TAK1), a protein within the MAPK pathway, may act as a molecular hub in signaling that plays a role not only in retinal development but also in inflammation through microglial cells that may help elucidate retinal diseases such as diabetic retinopathy (DR).

1.1 Development of the vertebrate eye

Oculogenesis is highly conserved in vertebrates and is characterized by three main phases that result in a mature, functional eye [5, 6]. Eye development is initiated early in embryogenesis shortly after gastrulation when three germ layers of the embryo are formed: the mesoderm, the endoderm, and the ectoderm[5, 6]. During gastrulation, the mesoderm induces the formation of the anterior neural plate from ectoderm. In late gastrulation, the central portion of the anterior neural plate is induced to form the structure that will eventually become the eyes, known as the eye field [5, 6]. The vertebrate eye develops from this eye field in the anterior of the neural plate. The neural plate evaginates to form the neural tube, followed by the eye field splitting to form the optic grooves. The optic grooves evaginate to form the optic vesicles. The optic vesicles then invaginate to form the optic cup, which forms the retina and the retinal pigmented epithelium (RPE) and the

optic stalk (Figure 1.1). Signaling from the evagination of the optic vesicles result in the formation of the lens placode that will eventually give rise to the lens. The optic stalk then narrows and marks where the optic nerve leaves the eye. The optic stalk connects the developing eye with the rest of the diencephalon. It is here that retinal ganglion cell axons will traverse the optic stalk to make synaptic connections with other regions of the brain [7].

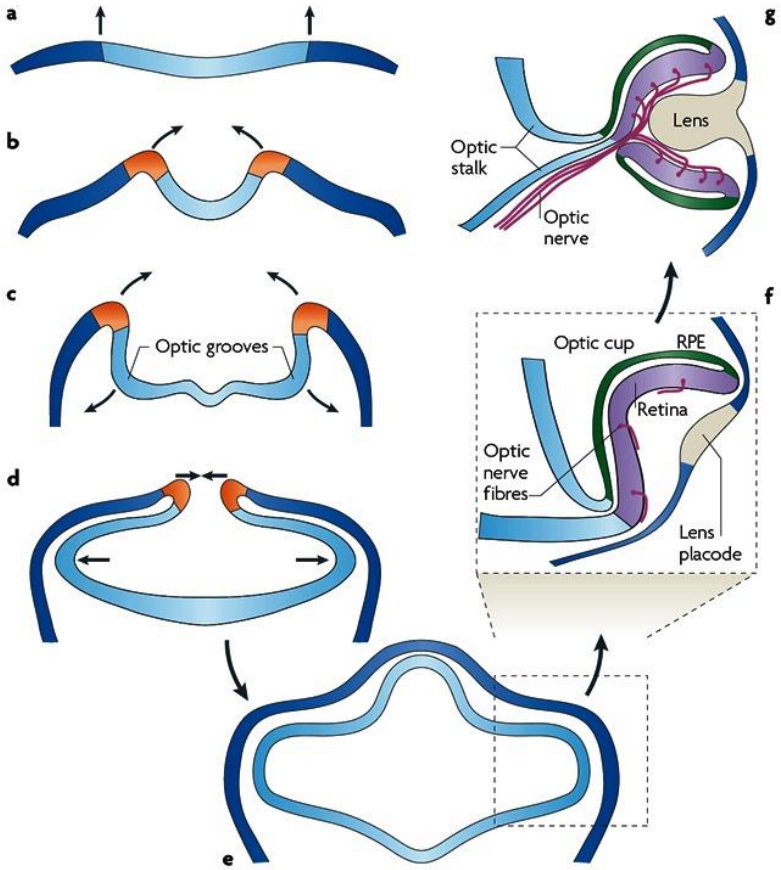

Figure 1.1 (a) The neural plate. (b) The neural plate folds to form the neural tube. (c) The formation of the optic grooves and they being to evaginate. (d) Optic vesicles bulge out as the folding continues. (e) The neural tube closes, and the formation of the lens begins. (f) Formation of the optic cup: the optic stalk, the RPE, and the retina. (g) The eyecup enlarges causing the choroid fissure to seal the optic cup. [8]

1.2 Retinal development

During retinogenesis, multipotent retinal progenitor cells (RPCs) are post mitotic precursors that undergo symmetric and asymmetric divisions to give rise to all the neuronal cell types and Müller

glia in the retina. The retinal cell types are born in a sequential manner, this sequential differentiation is what leads to the stratified mature retina. The competency model suggests that as development progresses, RPCs lose their ability to differentiate into certain cell types (Figure 1.2). Ganglion cells are the first-born cells, followed by horizontal, cone photoreceptors, and amacrine cells. The last to differentiate from progenitors are the rod photoreceptors and Müller glia.

Proliferation of RPCs is done via interkinetic nuclear migration which is where nuclei of cells move across the retina. This migration can occur close to the lens (vitreal) or close to the retinal pigmented epithelium (RPE) as progenitor cells enter different phases of the cell cycle. The cell cycle is split into interphase and mitosis. A cell's chromosomes undergo condensation before nuclear envelope break-down in G1 phase. In S phase, a cell replicates its DNA, afterwards, the cell prepares to divide as it enters G2 phase and divides or undergoes mitosis in M phase. As the nuclei of progenitors approach the completion of G1 phase, they migrate toward the vitreal surface where they enter S phase and initiate DNA synthesis. From here they migrate to the ventricular surface as they go from G2 into M phase. Differentiation of retinal cell types is the result of various signaling pathways and transcription factors which regulate cell type specification [9, 10]. For cells that remain in the cell cycle, activation of specific signaling pathways and cell cycle genes is necessary. Progression through the cell cycle and the phases within the cell cycle are controlled by cyclin dependent kinases (CDK). The cell cycle is positively regulated by cyclins and negatively regulated by CDK interactive protein (CIP) and kinase inhibitory proteins (KIP).

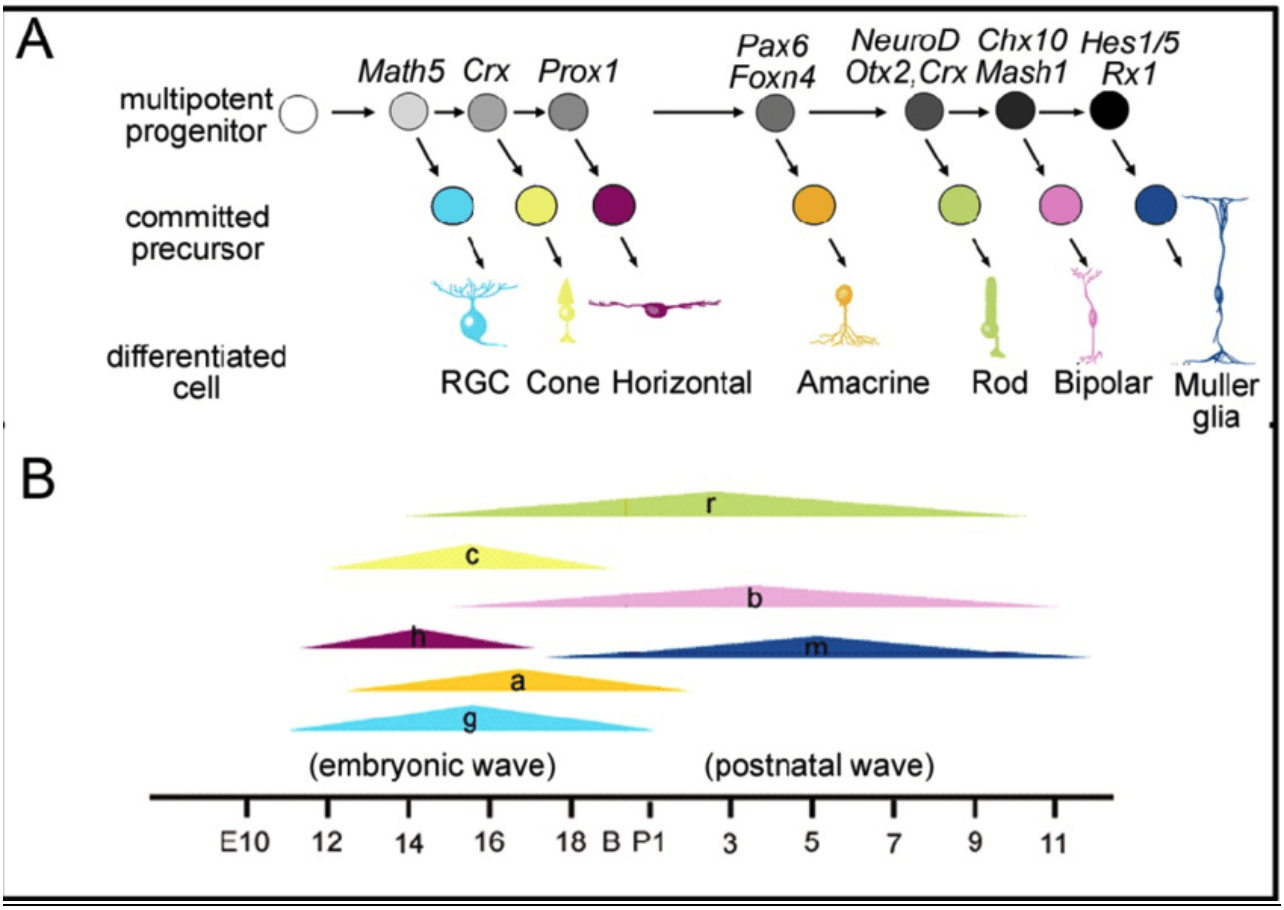

Figure 1.2 Sequential differentiation during retinal development.(a) Progenitor cells are restricted as development progresses, allowing for differentiation of various cell types. (b) Retinal differentiation occurs in two distinct waves that slightly overlap. [11]

1.3 The mature neural retina

The mature retina is a thin layer of highly organized tissue that lines the back of the eye. The retina is responsible for enabling vision by receiving light and converting that light into neural signals and passing it along to various parts of the brain that result in vision [12] (Figure 1.3). The mature vertebrate retina is made up of 3 main nuclear layers made up of neurons and 2 plexiform layers made up of synaptic contacts from adjacent layers [6]. The three main layers include the ganglion cell layer (GCL) made up of ganglion cells; the inner nuclear layer (INL) which is made up of bipolar, amacrine, and horizontal interneurons, and the outer nuclear layer (ONL) which is made up of rods and cones. Synapses between retinal ganglion cells and bipolar cells can be found in the

INL while synapses between the bipolar cell and photoreceptors can be found in the ONL. Ganglion cells also function outside of the nerve fiber layer; their axons extend out of the retina, through the optic nerve, to transmit converted signal outside of the eye to various parts of the brain [6]. Neurons are not the only cell type in the retina: glial cells (Müller glia, astrocytes, and microglia) are found throughout the retina. Müller glia, the primary glia of the eye, are found in the inner plexiform layer (IPL) of the retina while their processes extend through the entire length of the retina [6]. Astrocytes, specialized glial cells, can be found in the GCL and nerve fiber layer (NFL). As for microglia, they are the resident macrophages of the retina and are found in the plexiform layers [13].

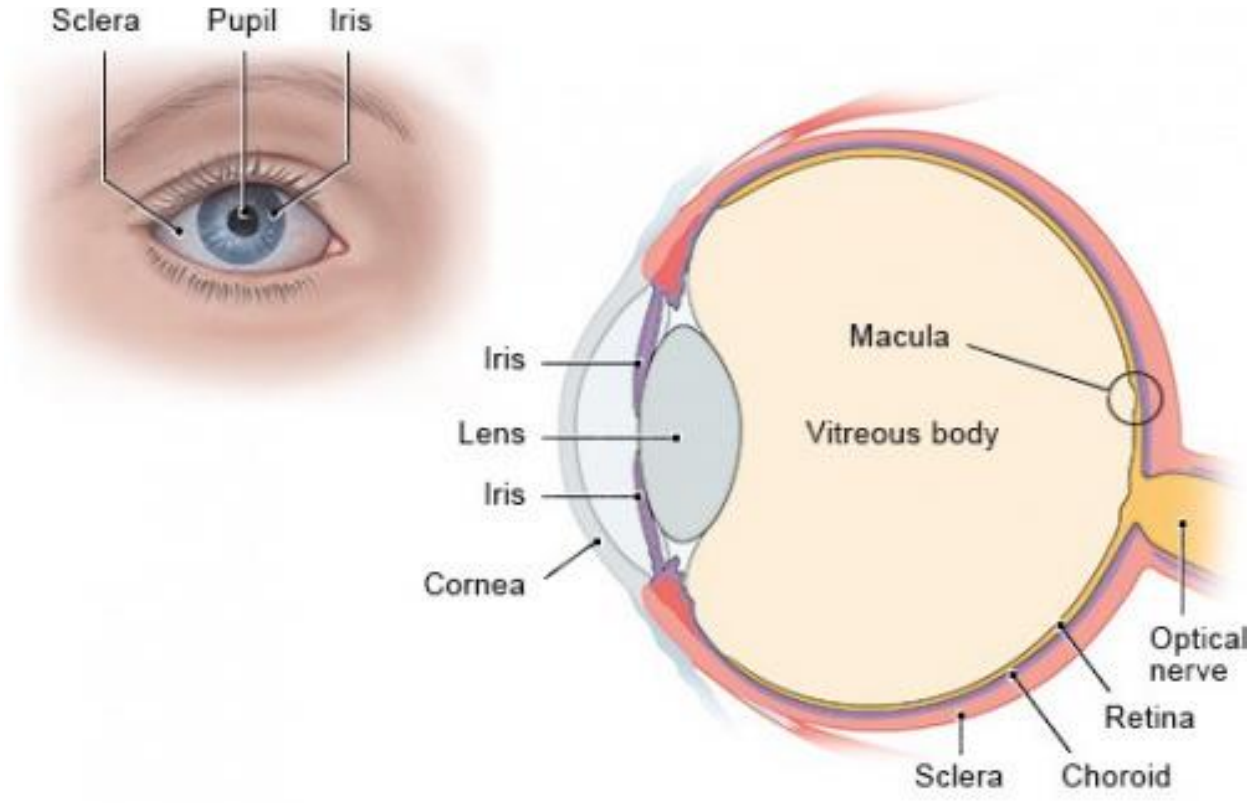

Figure 1.3 Retina location in the vertebrate eye[14]

1.3.1 Neuronal cell types

The retina is composed of 5 neuronal cell types: ganglion cells, amacrine cells, horizontal cells, bipolar cells, and photoreceptors (Figure 1.4). In vertebrates, ganglion cell neurons are typically the first cell type to differentiate. Ganglion cells migrate to the ganglion cell layer and their axons

extend through the optic disc and grow along glial cell end-feet in the optic nerve to secure their place there. A host of factors, including bHLH (basic helix-loop-helix) and its downstream factors are essential to the differentiation and survival of retinal ganglion cells [15, 16]. In some vertebrates, like chick, retinal ganglion cell axons are myelinated within the retina. However, most mammals have retinal ganglion cell axons that remain unmyelinated within the retina.

Amacrine cell differentiation overlaps with that of the retinal ganglion and the cells migrate to the INL. Displaced amacrine cells can also be found in the GCL. Currently, over 40 morphological subtypes of amacrine cells have been identified [8]. Amacrine cell's function, within the vertebrate retina, typically as inhibitory neurons. In vertebrates, they contain GABA or glycine, common inhibitory neurotransmitters when they are not nearby glutamatergic neurons, in which case can act in excitatory neurotransmission [17]. GABAergic amacrine cells make synapses with bipolar cells in the inner plexiform layer (IPL), aiding in creating a greater spatial and temporal recognition [18].

Horizontal cell birth overlaps with both amacrine and ganglion cell birth. Retinal horizontal cells are found in the INL of the retina, closest to the photoreceptors. They are interneurons that integrate signals between photoreceptors and are involved in lateral inhibition. Horizontal cells synapse onto photoreceptors cells. They serve as negative feedback to photoreceptors. This is due to horizontal cells depolarizing by the release of glutamate from photoreceptors in the absence of light; depolarization of horizontal cells leads to hyperpolarization of nearby photoreceptors. In light, less glutamate is released by photoreceptors which leads to hyperpolarization of horizontal cells, leading to polarization of photoreceptors.

Photoreceptors reside in the ONL of the retina and are split into two groups: rods and cones. Birth of cone photoreceptors overlaps with horizontal cells while rods are born later, overlapping with bipolar and Müller cells. Rods are found in far greater numbers in the retina compared to cones and are essential for vision in the absent of light. In humans and mice, there are 20 times more rods than cones, while in chick the ratio is about 6:1 [19]. Cones conversely provide vision in situations of bright light.

Bipolar cells are one of the last cells to be born in the retina. Bipolar cells are split into rod and cone bipolar cells based on their connections to either rods or cones. From here, they are also

categorized as ON of OFF bipolar cells. Bipolar interneurons also function to transmit signal to the ganglion cells. Bipolar cells are highly dependent on glutamate from Müller glia [20]. ON bipolar cells undergo depolarization due to the light in the rods while the OFF bipolar cells are hyperpolarized due to the light response in the cones.

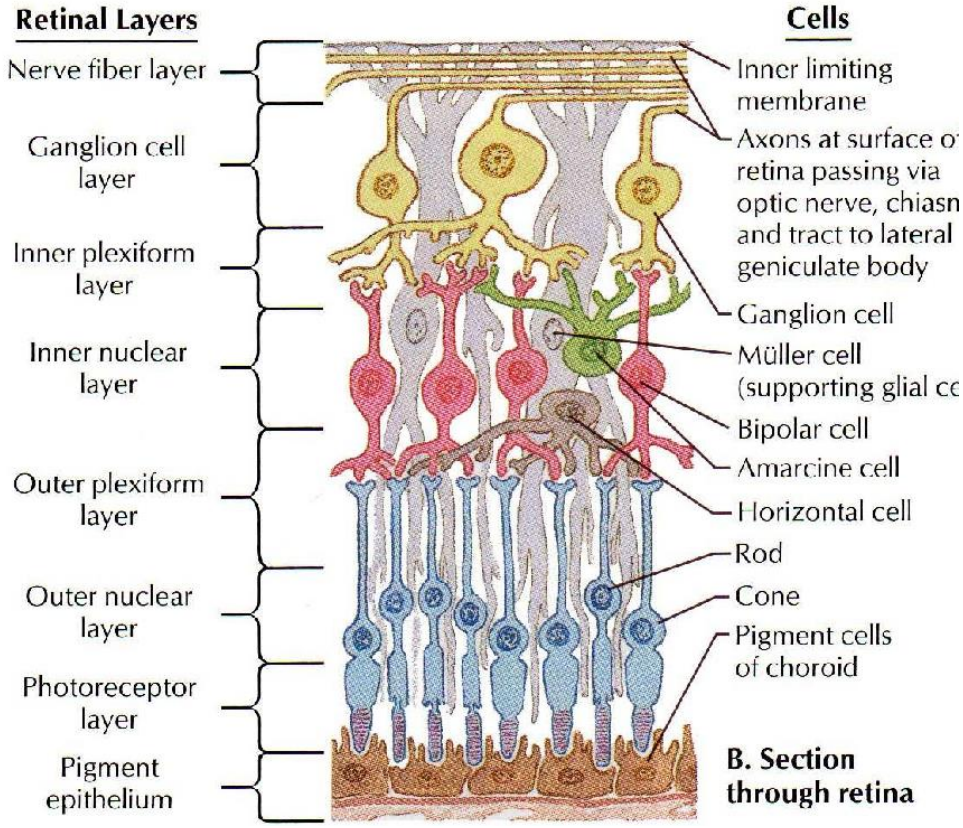

Figure 1.4 Layers of the mature vertebrate retina. Depicted are the main layers of the mature retina as well as the cells that reside in each one [21].

1.3.2 Retinal glia

Retinal glia play a key role in the regulation of neurotransmitters and their uptake. Retinal glia are necessary for neuronal protection and survival, formation and maintenance of the BBB, and homeostasis. They are classified into two groups: macroglia and microglia [22]. The macroglia include Müller glia and astrocytes. Müller glia are the last to differentiate from progenitor cells during retinogenesis along with rod photoreceptors and bipolar cells [23]. Müller glia are the predominant glia cell, making up about 90% of glial cells and span throughout most of the retina.

There is also evidence to suggest that Müller glia processes help aid other retinal cell migration and help guide differentiation [24]. Müller glia reside in the INL and their processes extend radially throughout all retinal layers while retinal astrocytes are found in the NFL [24]. Müller glia help provide structural support and line the blood vessels in the retina. Their end feet form the inner limiting membrane (ILM) of the retina and their outer processes form the outer limiting membrane (OLM). Müller glia cells help maintain homeostasis by taking up extra neurotransmitters, helping to stabilize the integrity of the retina, and maintaining the BBB in conjunction with the other glial cells: astrocytes and microglia. They are the only cells in the retina that exit then reenter the cell cycle in response to injury to surrounding neurons [25].

Retinal astrocytes work alongside Müller glia to help maintain homeostasis in the retina. Astrocytes, unlike Müller glia, do not originate from the retinal embryonic epithelium. It is thought that astrocytes come from mitotic precursors that traveled from the subependymal germinal layer of the brain to the optic nerve during development. From the optic nerve, astrocytes enter the retina through blood vessels [26]. Astrocyte processes cover blood vessels, aid in ion homeostasis, and are involved in synaptic pruning [26]. Astrocytic end feet aid in structural support for blood vessels, helping to maintain the BRB. Astrocytes have a stellate shape in the NFL and like Müller glia, their end-feet help form the ILM [26].

1.3.3 Microglia and inflammation

Microglia are resident macrophages of the retina that aim to maintain homeostasis. Microglial cells originate from embryonic yolk sac blood islands and migrate to the optic pit which then becomes the optic cup [27]. As innate immune cells, microglia have processes that extend from their cell bodies and survey their surroundings for debris and any indication of foreign bodies. Microglia are found throughout the retina: they reside in the NFL, GCL, IPL, and the OPL. Their development and survival is regulated by cytokine receptors and transcription factors [28]. As resident macrophages, microglia are key to regulating immunity and inflammation in the retina. Microglia express receptors such as toll-like receptors (TLRs), major histocompatibility complex (MHC), and cytokine and chemokine receptors that help them identify and respond to bacteria, viruses, and other foreign bodies [29]. When activated, like in the presence of oxidative stress or

hypoxia, microglia increase proliferation, and change morphology, changing into an amoeboid shape as they migrate to sites of injury [30]. Short inflammatory response leads to tissue repair and a return to homeostasis. However, chronic inflammation leads to sustained microglial activation and inflammatory response which can lead to neuronal damage and can potentiate diseases such as age-related neurodegeneration and glaucoma[30] (Figure 1.5).

Aside from their role in inflammation, microglia are also thought to play a role in the regulation of neuronal survival and programmed cell death during development as well as synaptic pruning[31]. There is also evidence that microglia are involved in angiogenesis and the integrity of the BRB. In angiogenesis, microglia help aid in the formation of blood vessels and their branching [32].

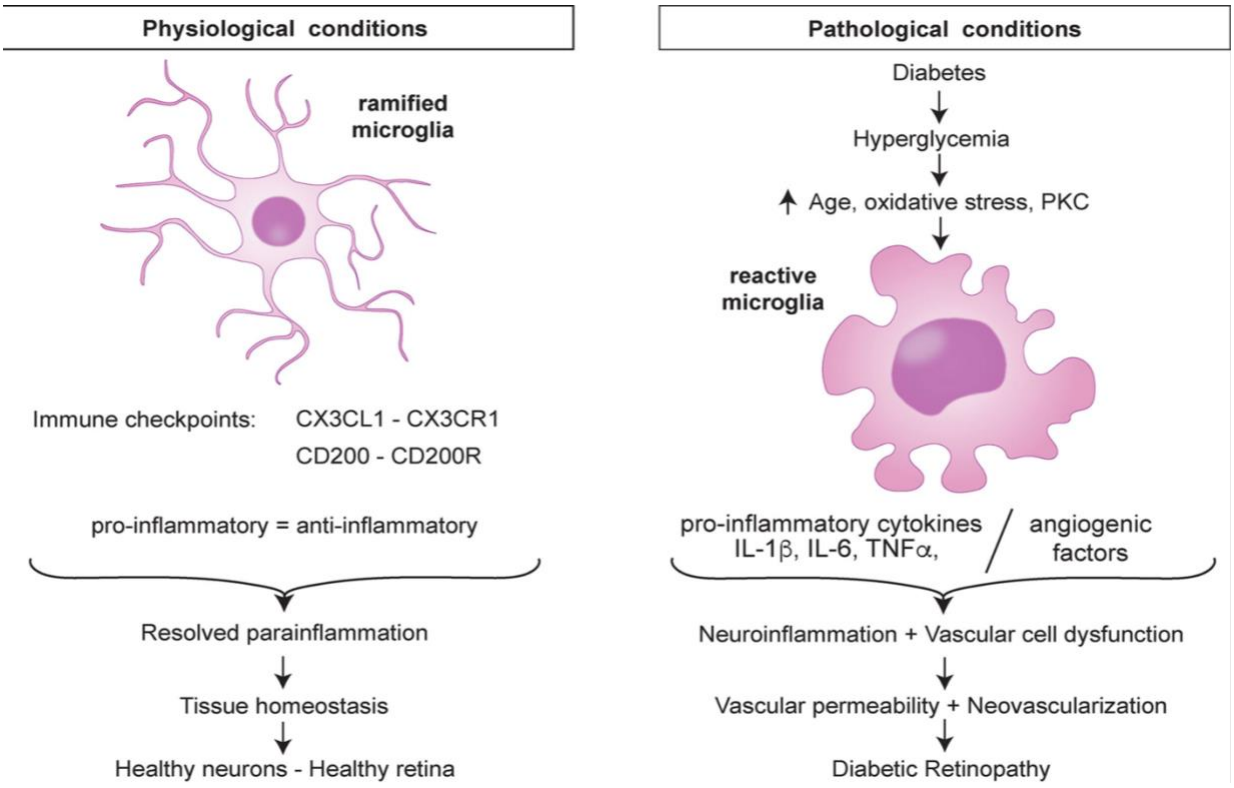

Figure 1.5 Microglia in homeostatic conditions (left) and in pathological conditions like diabetes (right) [33]

1.4 Retinal vasculature

The retinal vasculature supplies the retina with nutrients, oxygen, and structural stability. There are two main methods in which vasculature in the retina grows: angiogenesis and vasculogenesis. Mouse retinal vasculature develops like humans; during development, the inner vasculature grows and feeds from the optic nerve disc and spreads over the inner surface of the retina (vasculogenesis) [34] (Figure 1.6). The vasculature sprouting from the optic nerve is accompanied by astrocytes, which are also known to come in from the optic nerve. The vasculature follows the astrocyte migration until the retinal surface is covered. At this point, the vasculature is no longer associated with astrocytes as it branches out into the INL of the retina, creating parallel growth (angiogenesis) [34]. The retina also has a blood supply on the outside surface, supplied by the choroid, which supplies most of the total blood flow of the eye as well as nutrients and temperature control [34]. Retinal vasculature begins in utero, where the hyaloid vessels supply blood and nutrients to the retina and the eye during development [34]. Astrocytes that begin forming in the optic nerve during development express factors, such as vascular endothelial growth factor (VEGF), that triggers proliferation of endothelial cells [34]. These astrocytes and endothelial cells are key components of the BRB.

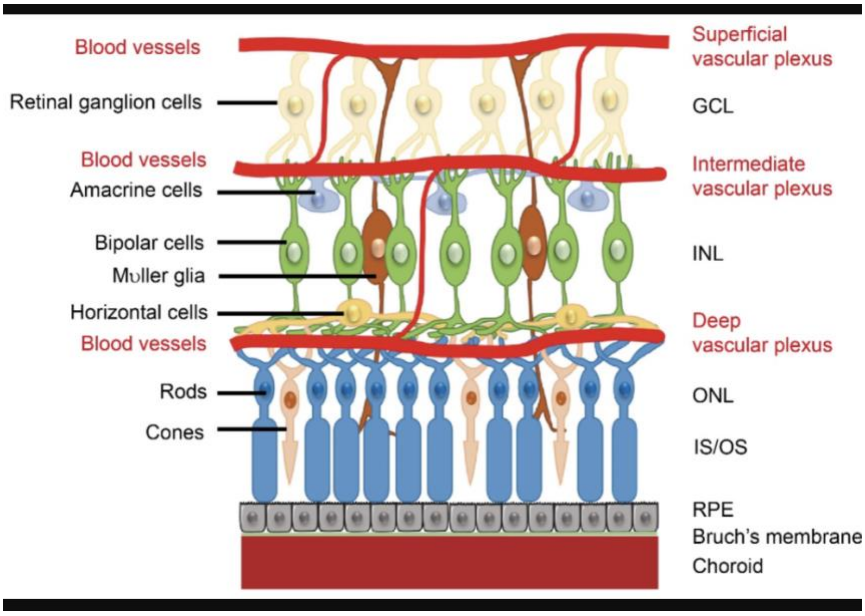

Figure 1.6 Vasculature of the mature vertebrate retina. From top to bottom: the superficial vascular plexus, the intermediate vascular plexus, the deep vascular plexus, and the choroid [35].

1.4.1 Blood retinal barrier

The BRB is a physical barrier that is essential to separating the circulating blood from the retinal vasculature and the extracellular fluid in the retina. This barrier is responsible for regulating ion and chemical flux in the environment surrounding the retina. The BRB is composed of retinal glia, the retinal pigmented epithelium, and cells that make up the vasculature. It is split into an inner and outer barrier: the outer barrier of the BRB is formed by the RPE while the inner barrier is formed by retinal glial end feet and cells of the vasculature. The inner barrier of the BRB is composed of interactions between endothelial cells, astrocyte and Müller glia end feet, and pericytes. Together, these cells form tight junctions that help regulate movement between the blood and the retina [36] (Figure 1.7). The outer barrier is essential to the regulation of movement of fluids and nutrients from the RPE to the photoreceptor layer (sub-retinal layer) [36].

Pericytes are essential to retinal homeostasis and the maintenance of the BRB. They are found along vasculature, embedded in the same basement membrane as endothelial cells [37]. While pericytes are present throughout the vascular network of the body, they are especially important when it comes to the CNS. In the CNS, pericytes help form the BRB and the BBB. They also aid in blood vessel formation and help control blood flow [37]. Most pericytes in the retina are recruited from the neural crest while a smaller amount are from the mesenchyme [37]. Pericytes are largely affected by the growth factors such as the platelet-derived growth factors (PDGFs). PDGF signaling regulates angiogenesis via interactions with receptors PDGFRα and PDGFRβ (Figure 1.8). Interactions between PDGF homodimers and their receptors are critical in the recruitment of pericytes to the vasculature and help maintain vasculature integrity and pericyte survival[38]. Endothelial cells secrete PDGF-BB, while pericytes express PDGFR-β, resulting in a codependency for survival [39]. Loss of PDGFR-B and/or PDGF-BB results in loss of pericytes and subsequent vascular abnormalities [40]. Disruption in the recruitment of pericytes can lead to weaking of the brain and retinal barriers and leaky vasculature; all of which result in serious disease states in the CNS. Damage to pericytes is an early hallmark sign of retinal disease, particularly in the case of diabetes.

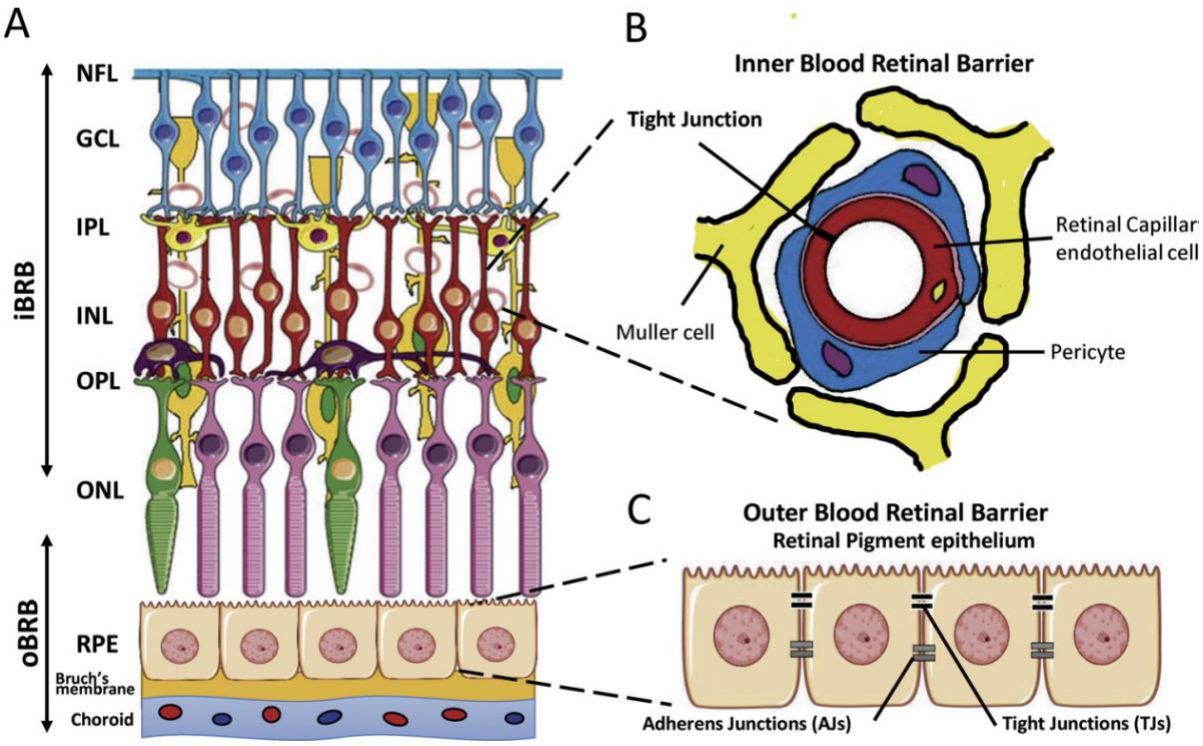

Figure 1.7 Inner and outer BRB. (a) The inner blood retinal barrier (iBRB) located in the main layers of the retina and the outer blood retinal barrier (oBRB) located in the retinal pigment epithelium (RPE). (b) A close up of the iBRB composed of tight junctions by endothelial cells, pericytes, and Müller glia. (c) A close up of the oBRB composed of both tight junctions and adherens junctions [41].

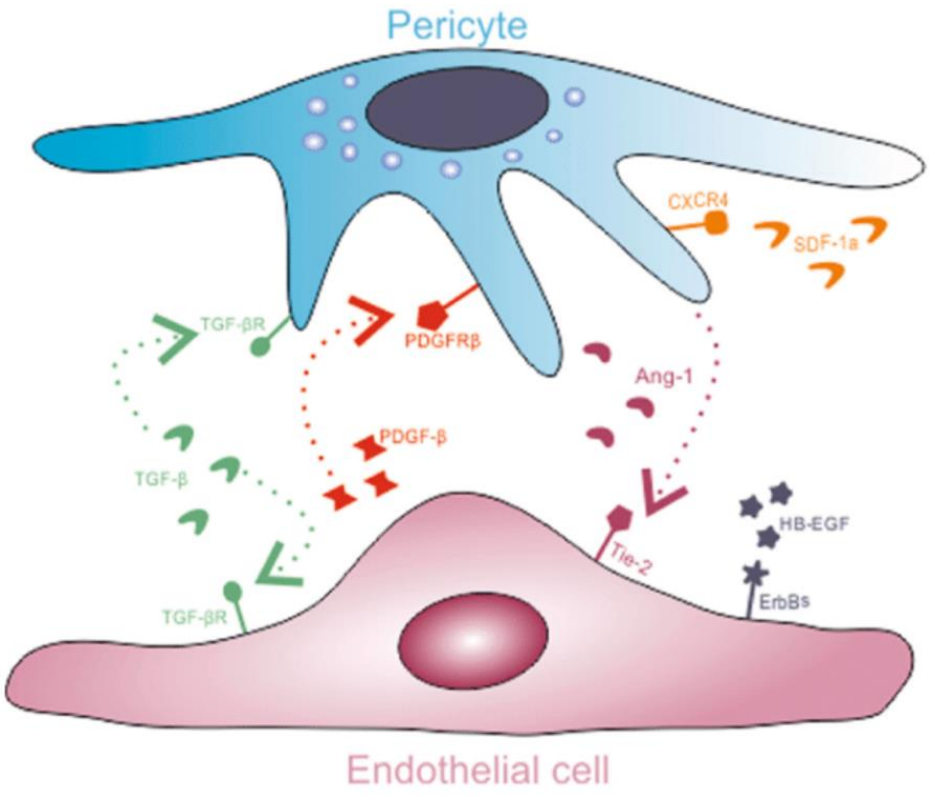

Figure 1.8 Pericytes are dependent on PDGF signaling for survival [42].

1.5 Diabetes

Diabetes is a metabolic disorder that is characterized into two main types: Type 1 and Type 2 Diabetes where there exists a defect in insulin secretion (type 1) or action (type 2) [43]. It is a disease that is a growing health concern not only in the United States, but globally. As of 2020, 34.2 million Americans have been diagnosed with diabetes, and as of 2018 88 million American adults have been diagnosed with prediabetes [44]. Globally, over 1.6 million deaths have been directly caused by diabetes as of 2018 [44]. Type 1 diabetes is usually diagnosed in children and is not known to have a cure, it makes up only 5-10% of all diabetic cases [44]. Meanwhile, over 90% of diabetic cases are type 2 diabetics, and while some subtypes of type 2 diabetes may be genetic, is largely considered preventable. One of the leading complications of diabetes is diabetic retinopathy (DR). It is the most common form of diabetic eye disease and is the leading cause of blindness in adults in the United States [45].

1.6 Diabetic retinopathy

Diabetic Retinopathy (DR) is a retinal disease and a major complication of diabetes. It is a disease that affects the vasculature, pericytes, and impacts vision capability. DR is categorized into four different stages in order of increasing neurodegeneration: mild non-proliferative, moderate non-proliferative, severe non-proliferative, and proliferative diabetic retinopathy [46] (Figure 1.9) The first stage is characterized by loss of pericytes, and the presence of microaneurysms, or swelling, in the retina. The presence of microaneurysms can lead to fluid leakage and pressure buildup in the retina, known as macular edema[46]. In the second stage of DR, moderate non-proliferative DR, there is the addition of hemorrhages, gliosis, lipid buildup (hard exudates), and dead cell debris (cotton wool spots) [47]. Severe non-proliferative DR is characterized by weakening of the blood vessels (venous beading) and there are areas in the retina that are no longer getting blood flow because of damage to the vasculature [47]. The final stage of the disease, proliferative DR, is characterized by neovascularization. In this stage, there is the formation of new vasculature, but due to a loss of pericytes, and consequently tight junctions of the BRB, these blood vessels are weak, leaky, and abnormal [47]. In the end stage of diabetic retinopathy, there is partial to complete vision loss and in some cases, retinal detachment [47].

The issue with a retinal disease like DR is that clinically, by the time a patient has symptoms, the disease state is already progressed far enough where damage has been caused. Research into this retinal disease has mostly been focused on later stages of DR to determine ways of alleviating symptoms and slowing down the progression of the disease. More recently, early stages of DR have been studied in an attempt to identify key changes early in diabetes that trigger the onset of the disease. Recent studies have shown that one of the first hallmarks of DR is the loss of pericytes [48]. While it has been found that these cells are lost, the methods in which this happens have yet to be uncovered [49]. Mechanisms relating to inflammatory stress have been proposed to explain the loss of pericytes and the onset of DR including oxidative stress, advanced glycation end products (AGEs), and a loss of PDGFB signaling [37]. The chronic inflammatory state of patients with diabetes aligns with the proposed inflammatory mechanisms.

Figure 1.9 Stages of Diabetic Retinopathy The 4 main stages of DR are shown with some hallmark symptoms that differentiate them compared to a normal retina. [50]

1.7 Mitogen activated protein kinase 1 (MAPK)

One mechanism that has shown potential for being involved in the onset of DR is the mitogen activated protein kinase (MAPK) family. MAPKs make up a set of signaling pathways that are essential to cell survival [51]. There are three main classes of MAPKs: extracellular-regulated kinase (ERK), p38, and c-junN-terminal kinase (JNK) that are regulated by a cascade of phosphorylation and are activated by extracellular stimulus[51]. ERK is important for neuronal functioning while JNK and p38 are important in apoptosis [51].

MAPK can also be activated by PDGF. When ligand PDGF-BB, secreted by endothelial cells, is binding to the receptor on pericyte cells, it triggers a phosphorylation cascade. A decrease in signaling of PDGF leads to death of pericytes and consequently endothelial cells as well [52]. Reactive oxygen species (ROS), reactive nitrogen species (NOS), and advanced glycation end products (AGEs), all of which can result from chronic inflammation due to diabetes, can lead to a decrease in PDGFRß signaling and lead to apoptosis. In the mouse retina, JNK was found to have a role in mediated apoptosis [53]. A study in rats found that inhibition of p38 in diabetic animals lead to inhibition of abnormalities associated in early stages of DR [54]. The activation of the MAPK/ERK signaling pathway has been used to study diabetic complications [55].

1.8 TGF-B activated kinase 1 (TAK1)

Recent studies have implicated TGF-B Activated Kinase 1, a MAP3K member or the MAPK family, as a key regulator of cell death [1]. Phosphorylation, or activation, of TAK1 requires the

adaptor protein TAK1 associated binding protein 1 (TAB1). TAB1 is also able to bind to p38. Phosphorylation of TAK1 at threonine 184, threonine 187, and serine 192 are required at the NH_2 terminal for activation of TAK1 [1].

TAK1 has been found to have a key role in maintaining tissue homeostasis. Activated TAK1 has been implicated in angiogenesis during embryonic development in mouse [56]. In various genetic mouse studies, TAK1 has been shown to control inflammation and cell death through downstream factors such as MAPKs and nuclear factor kappa-light-chain-enhancer of activated B cells (NFκB) [1]. Although NFκB has been shown to lead to proliferation, in type 2 diabetics with non-proliferative retinopathy, NFκB leads to pericyte apoptosis [57]. In mouse studies, dysregulation of TAK1 signaling showed tissue abnormalities similar to human disease pathogenesis [1]. TAK1 dysregulation has also been associated with cancers in various organs such as the kidney, liver, and colon [1, 58]. Deletion of TAK1 resulted in bone marrow and liver failure in mice as well as inactivation of both downstream JNK and NFκB signaling [59](Figure 1.10).

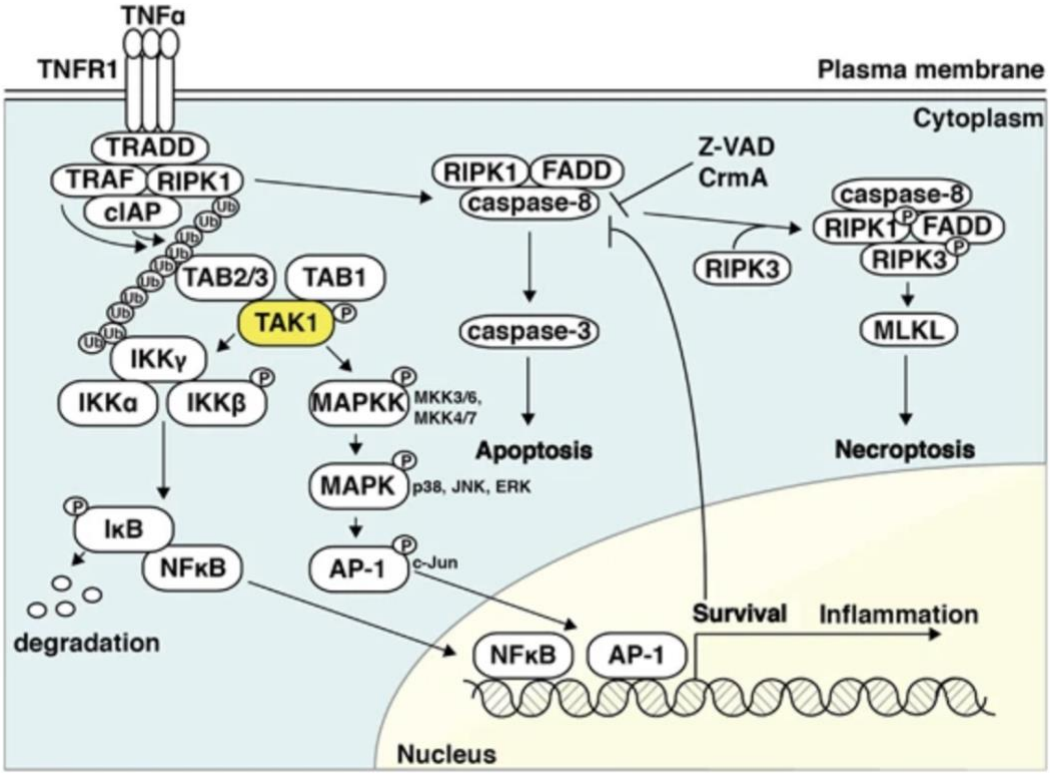

Figure 1.10 TAK1 downstream of TNF-α and upstream of proinflammatory factors [1].

Aside from its implicated role in inflammation and apoptosis, TAK1 was also studied in human retinal samples, the results of a study done in 2016 indicated a link between phosphorylation of TAK1 and human retinal pathology [60]. In a study looking at TAK1 specifically in microglia, TAK1 depletion negated post-ischemic neuroinflammation and apoptosis. Another similar study created a conditional deletion of TAK1 in microglia in mice and found not only a reduction in CNS inflammation, but also inhibition of the NFκB, JNK, and ERK1/2 downstream pathways [4]. These results suggest that TAK1 is important in pathology, particularly through mechanisms within microglial cells [61].

Previous studies in the Belecky-Adams lab found that although pericyte loss is happening as early as 3 weeks in genetic diabetic mouse models, inflammatory markers are not increased until about the 6-week mark. This suggests that inflammation affecting pericytes may not originate from the retina tissue itself. The BRB, where the pericytes reside, are surrounded by microglia. It is possible that TAK1 within microglia may be acting as a molecular hub that may be affecting pericytes and play a role in their loss in early diabetic retinopathy. The studies herein investigate the role of TAK1 in directing inflammation in diabetic retinopathy and in directing cell cycle progression in the developing retina. Regarding diabetic retinopathy, we hypothesize that TAK1 activity in retinal microglia increases the expression of secreted inflammatory factors that trigger the demise of retinal pericytes. In the developing retina, we hypothesize that TAK1 plays a role cell cycle progression by potentially signaling an increase in cell cycle length as development proceeds.

CHAPTER 2. TAK1 IN DIABETIC RETINOPATHY

2.1 Abstract

Diabetes is a disease affecting millions of people world-wide. Diabetic retinopathy (DR) is major complication of diabetes where 90% of Type 1 diabetics will develop DR and 60% of Type 2 diabetic will develop DR in the course of the disease. DR is one of the leading causes of blindness in the United States [62]. Current approaches to DR focus on treatments to alleviate symptoms and slow disease progression, particularly in the later stages of the disease. Events leading to the onset of the disease and the disease's early indicators have not been well studied and remain unclear. One indication of early DR is the loss or absence of pericyte cells, but the cause of their loss is unknown. Several factors are thought to be involved in their loss, however, the intracellular signaling pathways are not completely understood.

There are two general molecular structures involved in the detection of damage that affects the survival of an organism: damage-associated molecular pattern (DAMPs) and pathogen-associated molecular pattern (PAMPs). In DR, DAMPs can result in microglial activation [63]. In diabetes, receptor for advanced glycation end products (RAGE) and TLRs are the main DAMP and PAMP receptors present that when persistently elevated, can incite chronic inflammation. Previous studies have indicated that AGEs and other factors such as lipopolysaccharides (LPS), tumor necrosis factor α (TNFα) and bone morphogenetic protein 7 (BMP7) may play a role in regulating the expression of pro-inflammatory factors by acting as ligands at these receptors. Downstream of these main DAMP and PAMP receptors is TAK1. TAK1 has been implicated in regulation of inflammatory factors NFκB, JNK, and p38 in other parts of the body and in microglia in parts of the CNS but has not yet been studied in retinal microglia [3, 4]. TAK1 may be a critical component in the inflammatory pathway that acts downstream of multiple receptors and upstream of NFκB, a transcription factor that directly regulates upstream regulatory regions of pro-inflammatory factors [1, 2]. Studies from the Belecky-Adams laboratory have proposed that inflammation within the retina may be regulated by TAK1. We first wanted to test TAK1 in vitro to determine whether NFκB became activated in response to LPS, TNFα, and IFN-γ and whether this response could be inhibited by TAKinib. TAKinib is a potent inhibitor of TAK1. TAKinib functions by binding to

the ATP binding site of TAK1 via hydrophobic bonds. The nuclear localization of NFκB was used as a read-out of up-regulation of pro-inflammatory factors. In preparation for testing the role of TAK1 in an animal model of DR, I have also determined when pericytes are lost in streptozotocin (STZ)-treated C57BL/6 mice. Determining when pericytes are lost in STZ treated mice will allow me to be able to take the next step in creating an inducible knockout mouse model of TAK1 by determining the timepoint in which pericytes are lost in these mice. Mice treated with control vehicle or STZ will aid in determining if knockout of TAK1 in microglia reduces the presence of inflammation in the retina and if there is a change to pericyte health in these mice.

2.2 Introduction

Diabetes is a growing epidemic, affecting 34.2 million people in the United States and millions more worldwide [44]. Diabetes is characterized by increased blood glucose and chronic inflammation [44] and is thought to play a role in diabetic retinopathy, a major complication of diabetes. Nearly all type 1 diabetics and over 60% of type 2 diabetics will develop DR in the span and progression of their diabetes [44]. It is currently the leading cause of blindness in the United States. Chronic inflammation in diabetes is a direct result of excessive amounts of blood glucose in the body.

Of the two most common types of diabetes, type 1 diabetes is an autoimmune disorder in which the beta cells of the pancreas are destroyed, leading to insulin production being halted [43]. In type 2 diabetes, there is either insufficient insulin production and/or insulin resistance [43]. Both types result in an increase in blood glucose, or hyperglycemia, and patients of both suffer from DR. Despite such high prevalence of DR in diabetic patients, the mechanisms responsible for DR onset in diabetic patients is not known. Early DR signs include vascular changes to the retina but the major problem in DR is with the neurovascular unit (NVU) which includes pericytes, endothelial cells, macro and microglia, and neurons [64, 65].

Hyperglycemia or increased blood glucose has been shown to promote chronic inflammation due to the activation of inflammatory factors, AGEs, oxidative stress, and excessive protein kinase C (PKC) activation [66]. These various mechanisms can directly activate resident macrophages of

the retina, promote pericyte receptor death, and increase endothelial cell permeability. The effect of hyperglycemia on these cells directly affects the integrity of the BRB, thereby reducing retinal health. Chronic inflammation broadens the scope of potential culprits within the retina that are initiating DR to include: growth factors, cytokines, interleukins, and activation of microglia and other glial cell types. Chronic inflammation can be a direct result of gliosis and has also been shown to initiate astrogliosis as well [67]. Reactive gliosis is the activation of macroglia present in the CNS, including microglia, astrocytes, and Müller glia that can cause the formation of scar tissue and neuronal cell death [67].

Inflammation is a normal physiological response to injury and will often be short-lived and resolve itself. It often results in cytokine and chemokine secretion, changes in metabolism, and vascular changes. Chronic inflammation results from the continuous release of cytokines and chemokines. RAGE is present on many cells in the body including microglia and pericytes. AGEs have been shown to cause cell death and result in chronic inflammation [68] Some inflammatory factors such as IL-1β, TNF-α, and VEGF have been found to be increased in DR [69]. IFN-γ and IL-6 and other cytokines can directly cause dysfunction of glia. Microglial activation occurs in high glucose states found in diabetes and when activated, the microglia release proinflammatory factors [70]. Early signs of DR include microaneurysms and vascular changes and it has been found that one of the earliest changes to the eye in DR is the loss of pericytes [64]. The loss of pericytes lead to the changes seen in vascular integrity in the first category of DR. Multiple mechanisms have been proposed to explain the loss of pericytes in DR [71]. Both type 1 and 2 diabetes cause hyperglycemia which leads to oxidative stress [72, 73]. Hyperglycemia can also lead to an increase in pathways which increase NFκB and pro-inflammatory genes [74] and has also been linked to apoptosis [75].

Previous work from the Belecky-Adams laboratory suggest that chronic inflammation affected pericyte survival [76]. As previously mentioned, microglia are the resident macrophages of the CNS and are located near the vasculature. We hypothesized that TAK1, a kinase downstream of Toll-like receptors (TLRs)s, TNFα, and other factors and upstream of pro-inflammatory and pro-apoptotic factors, within microglia were responsible for exposing the neurovascular unit, including pericytes, to inflammatory factors. In order to approach this hypothesis, we first wanted to establish

that TAK1 can be activated by various factors in retinal microglia. I approached this by culturing microglia cells and treating with various activators of the TAK1 pathway: LPS, IFN-g, and TNFα. Immunocytochemistry was done to label for NFκB, a downstream factor of TAK1 that has been shown by many investigators to act as a central mediator of innate and adaptive immune responses[77]. NFκB is a transcription factor that does not require new protein synthesis to become activated. NFκB becomes activated through T or B cell receptors, and following a cascade of signaling components, eventually PKC becomes activated, activating NFκB, allowing it to be able to enter the nucleus. Once NFκB is in the nucleus, it is able to upregulate genes responsible for T-cell proliferation and development [78].

Cells immunolabeled with NFκB after activator treatment implicated the activation of TAK1 within those microglia. In addition to activator treatment alone, cells were also co-treated with activators and TAKinib, a specific inhibitor of TAK1 activation/phosphorylation, thereby inhibiting the cascade of downstream factors and NFκB translocation to the nuclear [58].The next step on testing this hypothesis is to test whether a loss of TAK1 would reduce inflammation in a disease state, DR, and whether this altered the changes to the neurovascular unit, such as pericyte loss. To perform those studies though, we first had to determine the time at which pericyte loss was occurring in an STZ-treated mouse. C57BL/6 mice were given an injection of STZ, a drug that kills off beta cells of the pancreas, mimicking a type 1 diabetic phenotype. The retinas of these animals were examined at various timepoints using immunolabeling in order to quantify pericytes in STZ treated animals compare to VEH treated littermates. The goals of these two preliminary studies was to explore 1) TAK1 can be activated and inhibited in microglia and 2) determine when early changes to the NVU are happening so that we can target the correct timepoints in TAK1 conditional knockouts. This will allow us to determine if the knockout of TAK1 in microglia can ameliorate any pericyte loss we see in C57BL/6 animals that were injected to have a type 1 diabetic phenotype. With these studies, I hypothesize that TAK1 acts as a molecular hub within microglia that is regulating inflammation in the early stages of DR that affects the NVU.

2.3 Materials and methods

2.3.1 Animals

C57BL/6J mice were purchased from Jackson Laboratories (Bar Harbor, ME). Animals were maintained in a temperature and humidity-controlled room with free access to food and water. All mice were housed in accordance with the Institutional Animal Care and Use Committee (IACUC) at Indiana University-Purdue University School of Science, Indianapolis.

2.3.2 Microglia cells

Briefly, microglial cells were isolated from the retinas of P0-P4 immmortomouse back crossed into C57BL/6J [79]. Retinas were digested in Trypsin/EDTA (5ml; 0.25% trypsin and 1mM EDTA; Thermo Scientific) for 5 min at 37℃. Retinas were then agitated using a pipette before 5ml of DMEM with 10% FBS was added to halt trypsin activity. Digested retinas were centrifuged at room temperature for 5 min at 400 × *g* and the supernatant aspirated. The remaining pellet was resuspended in microglia media made up of a 1:1 mixture of DMEM and F12 (Thermo Scientific) containing 44 U/ml of interferon- γ (R&D Systems, Minneapolis, MN) and 10% FBS. Microglia were then plated on a single well of a 6-well plate and maintained in a tissue culture incubator at 31°C and 5% CO_2. Cells were fed every 3-4 days until they were nearly confluent in 1-2 weeks' time. Once nearly confluent, media was removed from the plate and cells were rinsed with PBS containing 0.04% EDTA before 2ml of PBS with 0.04% EDTA was added to the plate and the plate was left on a multipurpose rotator at 100 rpm for 20-30 minutes at room temperature. The supernatant of the plate was placed in 3 ml of DMEM containing 10% FBS in a 15 ml tube which was then centrifuged at 400 × *g* for 5 minutes. The cells were then re-plated in microglia media and allowed to reach confluence before being expanded into 60-mm dishes. Flow cytometry analysis for F4/80 (eBiosciences; San Diego, CA) and keratin sulfate (Seikagaku Corporation; Jersey City, NJ) and immunocytochemistry was done to determine purity of the microglial cultures. The purity of the cultures was nearly 95% using both analyses.

Microglia were cultured in DMEM (Catalogue #D1152, Sigma-Aldrich, St. Louis, MO) containing 10% FBS and 44U/ml of murine recombinant interferon- γ (R&D Systems, Minneapolis, MN).

Cells were plated on a single well of a 6-well plate (BD Falcon) or a 100mm dish (BD Falcon) and incubated in a tissue culture incubator at 31°C and 5% CO_2. Cells had their media changed every 3 to 4 days and passaged every 5 to 7 days using .25% trypsin-EDTA (Sigma-Aldrich). Once reaching 60-80% confluency, microglial media was removed from the microglia, cells were rinsed with DMEM media and inoculated in non-FBS containing microglial media before being treated with factors and inhibitors. Cells were treated with either 1 µl/ml vehicle (PBS for IFN- γ for TNFα), 50 ng/ml of mouse interferon-gamma (IFN-γ; R&D systems), 10ng/ml of LPS (from E. coli; Sigma), or 50μM recombinant mouse TNFα (TNFα; abm) for 1 hour. Microglial cells were incubated with TNFα, IFN- γ, LPS, and vehicle for 1hr before being fixed and prepared for ICC. In the case where cells were treated with inhibitor, TAKinib (Sigma), cells were treated with 100pM of TAKinib for 24 hours before being treated with the above-mentioned concentrations of activators for 1 hour and fixed and prepared for ICC in the same manner.

2.3.3 Immunocytochemistry (ICC)

Following the treatment mentioned previously, microglial cells were fixed with 4% PFA for 30 minutes, rinsed with 1x PBS for 5 minutes twice, incubated with methanol for 10 minutes, and rinsed twice with 1x PBS for 5 minutes each. PBS was removed from each well of cells and a pap pen (Eletron Microscopy Sciences, cat#71310) was used to draw a square in each treated well of a 6 well plate and was allowed for dry for 10-15 minutes. Cells were blocked with 10% goat serum in 1x PBS with 0.25% triton X-100 for 1 hour at room temperature. Cells were then inoculated in primary antibody diluted in 1x PBS containing 0.25% Triton X-100 and 2% serum overnight at 4^{o}C. The following day, dishes were brought to room temperature before primary antibody was removed. Cells were rinsed with 1x PBS twice for 5 minutes each at room temperature before cells were incubated with the secondary antibody in 1x PBS for 1 hour at room temperature in the dark. After secondary antibody inoculation, cells were rinsed with 1x PBS twice for 5 minutes each, stained with Hoechst nuclear stain for 15 minutes, rinsed with 1x PBS twice for 5 minutes each, and then cover slipped using aqua mount and stored in the dark until imaged using a fluorescent microscope (All-in-One Fluorescence Microscope BZ-X800; Keyence).

Table 2.1 Table of Immunocytochemistry Antibodies

Antibody	Concentration	Catalog #	Vendor	RRID #
NFκB	1:100	PCRP-NFKB1-2B9	Developmental Studies Hybridoma Bank (DSHB	AB_2618888
IBA1	1:250	019-19741	FUJIFILM Wako	AB_839504
Alexa Fluor	1:500	A-11029	Invitrogen`	AB_138404

2.3.4 Streptozotocin treatment and animal monitoring

Male C57BL/6J mice were used for experimentation. Female mice were excluded because they have been found to be more resistant to streptozotocin (STZ), requiring 50% more STZ per kg of body weight compared to males [80]. Male mice of 8 weeks of age were fasted overnight by removing food at 5pm until the following morning. Citrate buffer was prepared in a conical tube (Corning) and adjusted to a 4.0 pH using 1M NaOH and filter sterilized before putting on ice. STZ in solution has a half-life of 15-40 minutes so STZ-citrate buffer solution was made immediately before injections to preserve ability to induce diabetes. Male mice were injected intraperitoneally with STZ [81] at a dose of 100mg/kg using syringe with a 29 gauge needle (EXEL). In control animals, citrate buffer was injected at the same volume used for the STZ group. Mice were given 10% sucrose water post-injection to prevent sudden hypoglycemia that was changed out for fresh water the day following injection. Mice were housed in cages with extra absorbent bedding. A reading of fed blood glucose ≥250mg/dL was considered diabetic. If STZ injected mice did not have a blood glucose reading of ≥250mg/dL by the 5^{th} day, they were euthanized, and the procedure was redone on a new animal. Blood for blood glucose reading was obtained from the tip of the tail and body weight and blood glucose was monitored the day before injection, the day of injection, and daily for 5 days post injection to ensure reading above 250mg/dL. This was all done at the same time of day, in the morning. Mouse blood glucose reading was also taken at the time of sacrifice, which were also done in the morning (Table 2.2). Mice that experienced complications and extreme weight loss or signs of distress were not included in the study and were consequently euthanized using CO_2 followed by secondary method of euthanasia: cervical dislocation.

Table 2.2 Blood Glucose Readings

Group	Sex	Blood Glucose day before injection (mg/dL)	Blood Glucose at time of sacrifice (SAC) (mg/dL)
4 week STZ (n=3)	M	140 ± 7	564.5 ± 10.5
4 week VEH (n=3)	M	159.5 ± 13.5	174.5 ± 2.5
6 week STZ (n=4)	M	164 ± 3	265.5 ± 1.5
6 week VEH (n=3)	M	161.5 ± .5	136.5 ± 15.5
10 week STZ (n=2)	M	127.5 ± 8.5	331 ± 16
10 week VEH (n=2)	M	95.5 ± 1.5	130.5 ± .5

2.3.5 Retinal flat-mount immunohistochemistry

Eyes were dissected from mice that were euthanized using CO_2 and cervical dislocation. Eyes were placed in 4% PFA for 30 minutes on ice and then rinsed with 1x PBS several times. Retinas were removed using a dissecting scope and tools and placed in methanol (MeOH) at -20℃ until ready for immunohistochemistry. Retinas were rinsed in 0.5% Triton X-100 in 1x PBS (PBST) twice for 10 minutes. Then they were placed in blocking solution made up of 10% serum in PBST-0.5% overnight at 4°C. Retinas were rinsed once with 0.5% PBST for 10 minutes before incubating with primary antibody in blocking solution at 4°C. For retinal processing, retinas were incubated with primary antibody for 5 days. Retinas were then rinsed with 0.5% PBST three times for 5 minutes each on a shaker before being incubated with secondary antibody in blocking solution overnight at 4°C. Retinas were rinsed with 0.5% PBST 3 times for 5 minutes each on a shaker before being mounted on slides with aqua mount and cover slipped (adapted from Buhr et al).

Table 2.3 Table of Immunohistochemistry Antibodies

Antibody	Concentration	Catalog #	Vendor	RRID #
NG2	1:400	AB5320	Millipore	AB_11213678
IB4	1:500	I21411	Life Technologies	AB_2314662
Alexa Fluor	1:500	A11037	Life Technologies	AB_2534095

2.3.6 Retinal pericyte cell counts

For retinal flat mounts, retinas were divided into two regions. The inner region of the retina was determined from 0-1000µm from the optic nerve head and the outer region from 1001-2000µm from the optic nerve head. Images using a fluorescent microscope (All-in-One Fluorescence Microscope BZ-X800; Keyence) were taken of 3-5 sections within each region. Images were analyzed using NIH Image J. Statistical tests include one-way analysis of variance (ANOVA) with a Tukey's multiple comparison post-hoc tests with probability levels of 0.05, 0.01, 0.001.

2.3.7 Microglia cell counts and statistics

For microglial cell counts, 15-20 regions were imaged within a single well using a fluorescent microscope (All-in-One Fluorescence Microscope BZ-X800; Keyence). Each treatment group (n=2) was done in triplicates in a 6 well plate (n=1). Quantification was done using NIH Image J. Error bars of averages n=6, 3 technical replicates and two biological replicates are shown in black. Statistical tests include one-way analysis of variance (ANOVA) with a Tukey's multiple comparison test with probability levels of 0.05, 0.01, 0.001.

2.4 Results

2.4.1 NFκB translocation to the nucleus was increased in microglia cells treated with TNFα

Current literature has not explored TAK1 and its role within microglial cells in regard to inflammation in the eye. To approach our hypothesis that NFκB can be activated in microglia, various factors known to activate NFκB, a downstream factor of TAK1 were used to treat microglia. TNFα has been shown to recruit TAK1, leading to NFκB activation [82]. Microglia cells were cultured and treated with 50μM of mouse recombinant TNFα and immunolabeled for NFκB, a downstream factor of TAK1 (Figure 2.1A). In addition to TNFα treatment, microglia were also treated with TNFα in the presence of TAKinib, an inhibitor of TAK1 phosphorylation which is needed to activate downstream factors. Analysis of NFκB co-localization with Hoechst in vehicle treated cells showed a mean of 42.05% ± 3.98%. In cells treated with TNFα, NFκB$^+$ cells were 77.40% ± 3.98% and when cells were treated with TNFα and inhibitor, 34.50% ± 3.56% of cell were labeled NFκB$^+$ (Figure 2.1B).

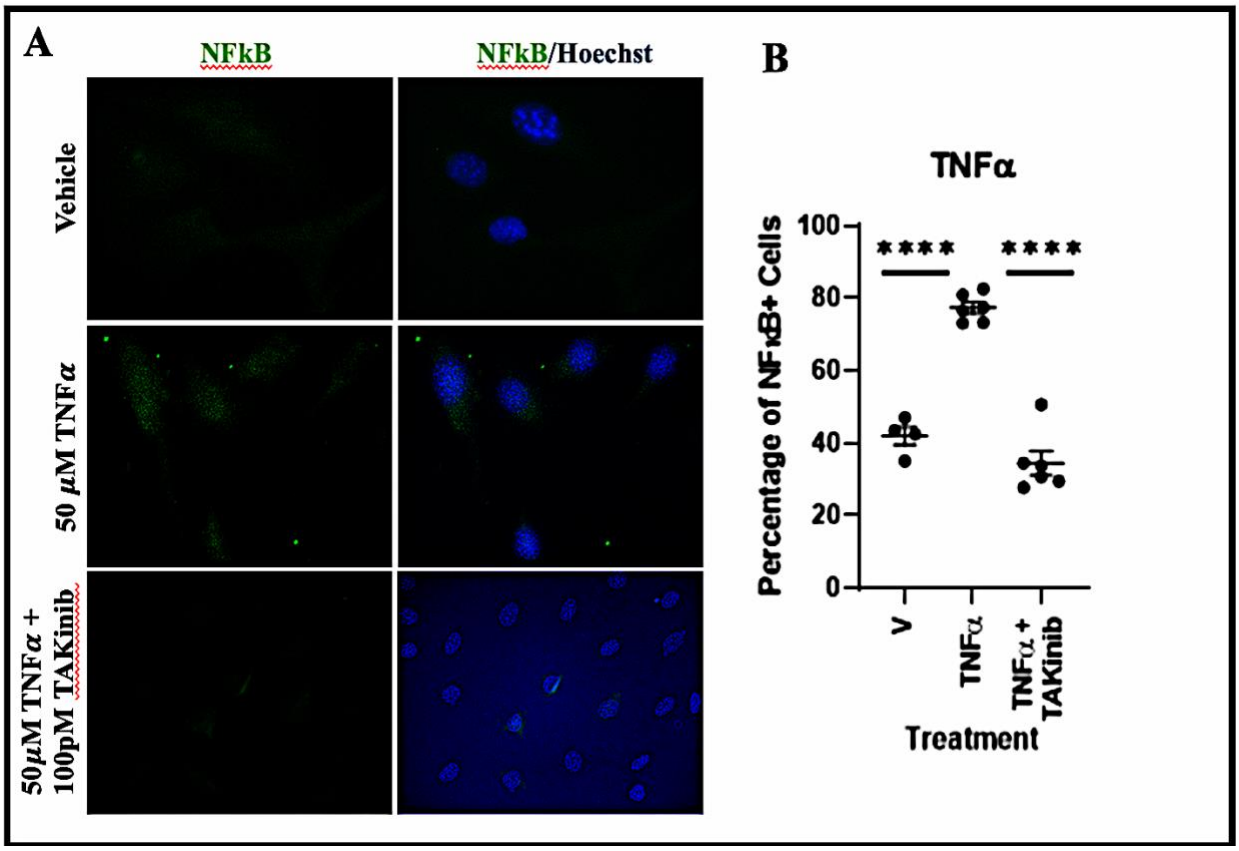

Figure 2.1 NFκB translocation to the nucleus is increased by TNFα in microglia cells and this translocation is reduced by TAK1 inhibition. A) Retinal microglia were grown in 6 well plates, treated with vehicle, 50 mM TNFα, or 100pM TAKinib + 50 mM TNFα. Cells were immunolabeled using nuclear factor kappa-light-chain-enhancer of activated B cells, NFκB, and a nuclear marker, Hoechst. Each 6 well plate was split into two, with a triplicate of vehicle treated, and a triplicate of the treatment group. 15-20 regions of each well were imaged at 40x magnification using a fluorescent microscope, and cell counts of vehicle and treatment triplicates were averaged for each plate (n=2). B) Quantification of NFκB+ cells were graphed using excel with SEM bars shown in black. Statistical significance was determined using a one-way analysis of variance (ANOVA) with a Tukey's multiple comparison test (**** $p<0.0001$).

2.4.2 Treatment of microglia showed a change in NFκB+ cells in the presence of IFNγ and IFNγ + TAK1 inhibitor

Figure 2.1 showed that TNFα treatment of microglia increased translocation of NFκB to the nucleus and that this translocation appears to be inhibited by a TAK1 inhibitor. In order to explore my hypothesis that inhibition of TAK1 can prevent NFκB translocation to the nucleus, IFNγ was used as a treatment for cells. IFNγ is a known immune interferon and has been shown to activate

NFκB through the autophagy pathway. Microglia cells were cultured and treated with 50ng IFNγ and cells were then immunolabeled for NFκB (Figure 2.2A). In addition to 50ng IFNγ treatment, microglia were also treated with IFNγ in the presence of TAKinib, an inhibitor of TAK1. Vehicle treated microglia resulted in 41.21% ± 6.06% cells labeled NFκB^{+}. Cells treated with IFNγ showed a 74.35% ± 6.0% of NFκB^{+} labeled cells. When cells were treated with IFNγ plus the inhibitor, number of cells labeled with NFκB^{+} was 33.18% ± 5.381% (Figure 2.2B).

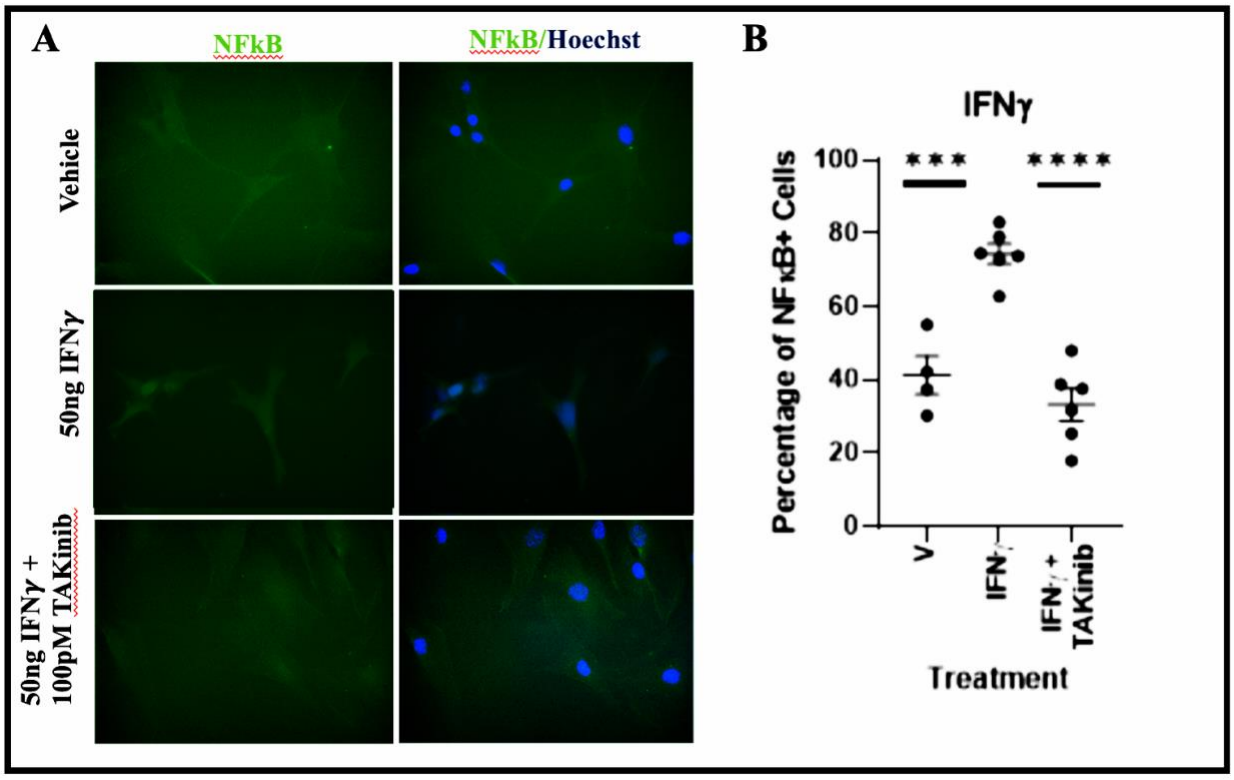

Figure 2.2 NFkB translocation to the nucleus is increased by IFNg in microglia cells and this translocation is reduced by TAK1 inhibition. A) Retinal microglia were cultured in 6 well plates, treated with vehicle, 50ng IFNγ, and 100pM TAKinib + 50ng IFNg. Microglia were immunolabeled using NFκB. Each 6 well plate was split into two, with a triplicate of vehicle treated, and a triplicate of the treatment group. 15-20 regions of each well were imaged at 40x magnification using a fluorescent microscope, and cell counts of vehicle and treatment triplicates were averaged for each plate (n=2). B) Quantification of NFκB+ cells were graphed using excel with SEM error bars shown in black. Statistical significance was determined using a one-way analysis of variance (ANOVA) with a Tukey's multiple comparison test (**** $p<0.0001$).

2.4.3 Treatment of microglia showed a change in NFκB+ cells in the presence of LPS and LPS + inhibitor

The final activator we wanted to use to treat microglial cultures was LPS. LPS is categorized as an endotoxin and has been shown to activate multiple protein kinases through TAK1 [83]. In a similar fashion to previous activators used, microglia cells were cultured and treated with vehicle, 10ng LPS, or 10ng LPS + TAKinib. Cells were then immunolabeled for NFκB (Figure 2.3A). Vehicle treated cells had 27.6% ± 3.01% cells have NFκB$^+$ labeling in the nuclei. LPS treated cells on the other hand had 66.46% ± 3.0% of cells with NFκB$^+$ labeling in the nuclei. In LPS with TAKinib treatment, only 31.77% ± 3.0% of total cells were labeled NFκB$^+$ (Figure 2.3B).

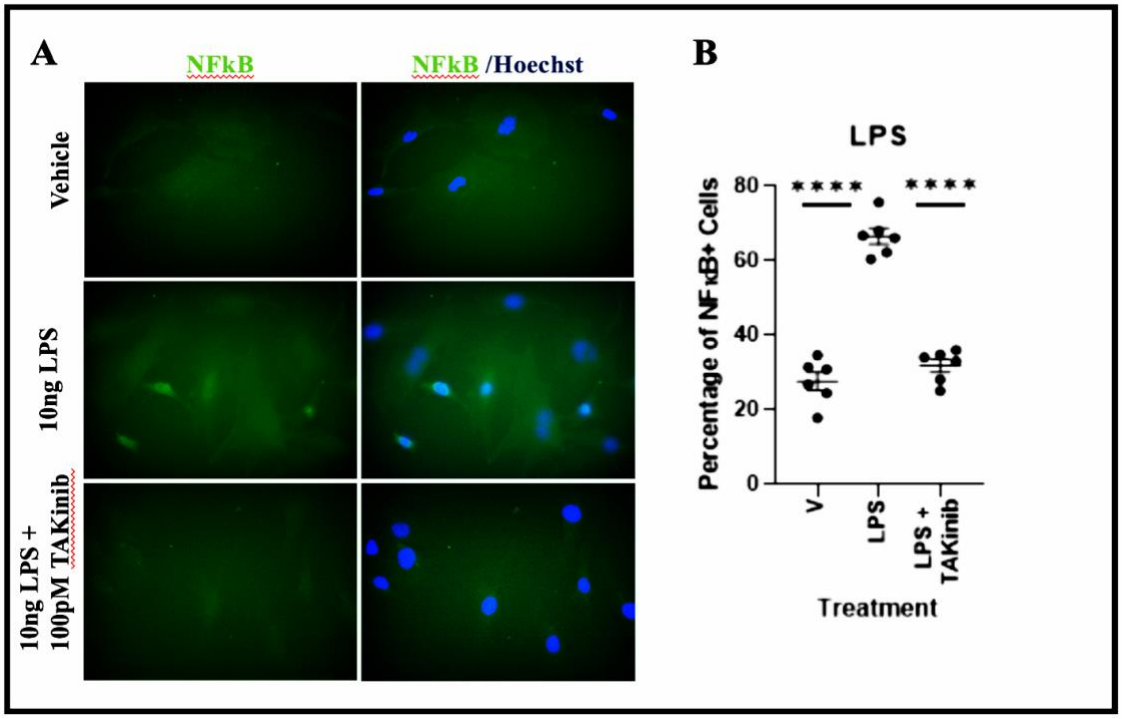

Figure 2.3 **N**FkB translocation to the nucleus is increased by LPS in microglia cells and this translocation is reduced by TAK1 inhibition**.** A) Retinal microglia were cultured in 6 well plates, treated with either vehicle, 10ng LPS, and 100pM TAKinib + 10ng LPS. Microglia were immunolabeled using NF*κ*B. Each 6 well plate was split into two, with a triplicate of vehicle treated, and a triplicate of the treatment group. 15-20 regions of each well were imaged at 40x magnification using a fluorescent microscope, and cell counts of vehicle and treatment triplicates were averaged for each plate (n=2). B) Quantification of NF*κ*B+ cells were graphed using excel with SEM error bars shown in black. Statistical significance was determined using a one-way analysis of variance (ANOVA) with a Tukey's multiple comparison test (**** $p<0.0001$).

2.4.4 Pericyte loss was evident in the STZ model of diabetes at 4 weeks

In order to determine when the neurovascular unit was being affected in a diabetic animal model, the progression of retinal pericyte loss in STZ-treated mice was determined. Control animals for STZ-treated mice were littermates that were given intraperitoneal injections of corn oil not containing STZ. Following injection of STZ, animals had a blood glucose reading every day for five days until blood glucose read >250mg/dL and that was then denoted as day 1. Control animals were aged from date of corn oil injections. 4, 6, and 10 weeks from the day of injection or day of becoming diabetic, animals were sacrificed. When animals were sacrificed, retinas were taken and fixed for retinal flat mounts that were then immunolabeled for pericyte marker neural/glial antigen 2 (NG2). 4 week vehicle animals had a mean of 36.83 (± 1.65; n=3) pericytes while 4 week STZ animals had a mean of 33.62 (± 2.1; n=3) pericytes in an area of 520 μm^2. Pericyte at 6 weeks STZ had a mean of 25.46 (± 1.8; n=4) compared to 6 week vehicle which had 33.14 (± 2.4; n=3) pericytes per 520 μm^2 area. In 10 week old animals, STZ treated animals there were 16.19 (± 1.6; n=2) pericytes compared to vehicle treated at 10 weeks which had 29.42 (± 3.2; n=2) pericytes per 520μm^2 area. When comparing STZ treated animals to their vehicle treated controls, there is a downward trend, with statistical significance presence between STZ and vehicle at 6 weeks and at 10 weeks. STZ-treated animals at 6 and 10 weeks were both significantly lower in number of pericytes compared to their wildtype littermates. The 4 week STZ-treated animals did not have a significant decrease in pericyte number compared to the 4 week wild type although there does appear to be a trend for a decrease in pericyte number at this timepoint. When a two-way ANOVA was done, the results showed variability within animal ages in both treatment groups (Figure 2.5). When comparing vehicle treated animals, there is a statistically significant decrease from 4 week to 6 week and from 4 week to 10 week with a p value of 0.0358 and 0.0006 respectively. When comparing STZ treated animals across the three varying ages, there is a downward trend is pericyte number, with statistical significance present between 4 week STZ and 6 week STZ, 6 week STZ to 10 week STZ, and 4 week STZ to 10 week STZ.

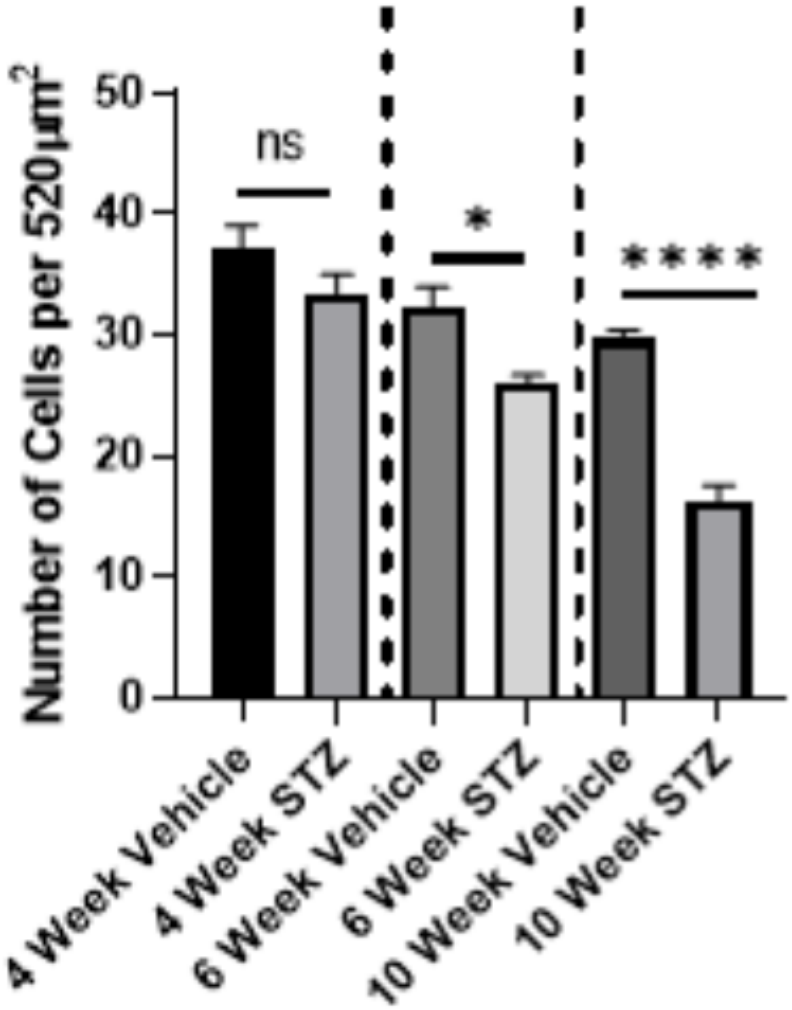

Figure 2.4 Retinal Pericytes decrease in an STZ model of Diabetic Retinopathy. Retinal flatmounts from 4, 6, and 10 week mice from WT or STZ treated animals were immunolabeled for pericytes using neural glial antigen 2 (NG2) marker. Retinas were imaged in two regions, 0-1000µm from the optic nerve head and 1001-2000µm from the optic nerve head. Within each region, 3-5 images were taken and cell counts were done using NIH image J and then averaged. Quantification of NG2+ cells from each region was graphed using Graphpad Prism. Statistical significance was determined using a one-way analysis of variance (ANOVA) with a Tukey's post hoc multiple comparison test (**** $p<0.0001$).

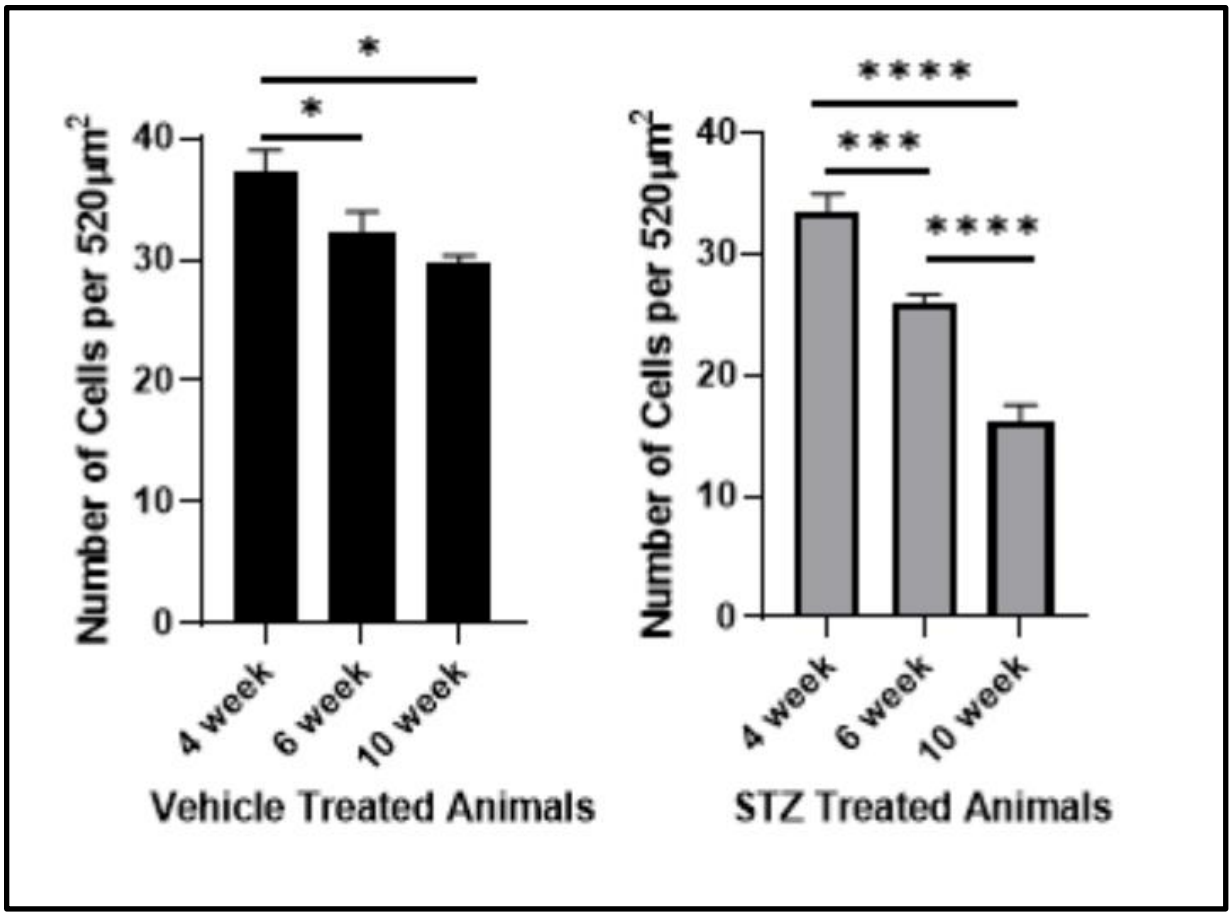

Figure 2.5 Retinal Pericytes at varying ages. Two-way Anova analysis of quantified NG2+ cell in vehicle and STZ treated animals from 4, 6, and 10 week mice. Statistical significance was determined using a two-way analysis of variance (ANOVA) with Tukey's post hoc multiple comparison test (**** $p<0.0001$).

2.5 Discussion

2.5.1 Summary

The role of inflammation in diabetic retinopathy is not well understood but is known to affect every level of the neurovascular unit. Compromising the integrity of the neurovascular unit leads to leaky vasculature, loss of retinal neurons, and gliosis in microglia and macroglia. The role of TAK1 was explored in murine retinal microglial cultures by looking at the transcription of pro-inflammatory factor NFκB, known to be activated by multiple signaling pathways: TNFα, LPS, and IFNγ. Treatment with TNFα, LPS, and IFNγ showed an increase in translocation of NFκB to

the nucleus. This translocation of NFκB to the nucleus was shown to be inhibited when cells were treated in the presence of a TAK1 inhibitor.

In vivo work showed that inducing a type 1 diabetic phenotype in mice using STZ resulted in loss of pericytes at 6 weeks post diabetic induction. Loss of pericytes steadily decreased from 4 week to 6 week to 10 weeks post type 1 diabetic induction compared to vehicle treated controls.

2.5.2 TAK1 activation leads to NFκB nuclear localization in retinal microglia cultures

Retinal microglia are the resident macrophages of the retina and when cytokine and chemokines are secreted, chronic inflammation can result. PAMPs and DAMPs have been shown to be upregulated in DR so we chose to treat cells with various ligands to activate receptors in order to get an inflammatory response. Treatment with these ligands was used to determine if retinal microglia would activate the NFκB pathway by labeling the translocation of NFκB to the nucleus. AGEs have been found to be increased in DR but we were unable to treat microglia with these since they are not commercially available. Few studies exist of lab made AGEs but the process is complicated, requiring long incubation times and need characterization to ensure they indeed function like AGEs. Although we could not treat with AGEs, we could treat with other ligands that are known to activate the RAGE receptor, such as HMGB1, but this also activates TLRs.

In-vivo studies I conducted in retinal microglia determined that when looking at pro-inflammatory activators and their effect on TAK1, there was an increase in NFκB+ cells when immunolabeling was done on cells that were treated with various activators: LPS, IFNγ, and TNFα. TNFα is a well-known pro-inflammatory factor that has been linked to chronic inflammation in diabetes, particularly type 1 diabetes. TNFα is also known as one of the best activators of the NFκB pathway [84].

Treatment of retinal microglia with TNFα had a statistically significant increase compared to vehicle treated cells. When these cells were treated with the TAK inhibitor, TAKinib, first and then TNFα, there was no significant change in NFκB+ labeled cells compared to vehicle treated wells. Retinal microglial cultures treated with LPS yielded similar results, showing a statistically

significant increase in NFκB+ cells when immunolabeling was done. When retinal microglia were treated with TAKinib followed by LPS, there appeared to be no change in number of NFκB+ cells compared to vehicle treated cells. While TNFα, LPS, and IFNγ have all been found to activate the NFκB pathway, only TNFα and LPS have been linked to working through the TAK1 pathway [77, 85].

IFNγ on the other hand, has not previously been implicated to working through the TAK1 pathway as a way of activating downstream factor NFκB. IFNγ has previously been shown in oligodendrocytes to activated NFκB through pancreatic endoplasmic reticulum kinase (PERK) [86]. When retinal microglia cultures were treated with IFNγ, there was an increase in the number of NFκB+ cells, which is expected. However, when retinal microglia cultures were treated with TAKinib followed by IFNγ, there is a decrease in number of NFκB+ cells compared to cells that received just IFNγ treatment, yielding a result similar to vehicle treated. It is possible that IFNγ can also work through the TAK1 pathway to activate downstream NFκB. Scarneo et al stimulated THP-1 macrophages with IFNγ and LPS and when co-treated with TAKinib, found that there was a reduction in TNF and IL-6 secretion, but did not look at NFκB [58]. It is also possible that TAK1 acts directly on NFκB regardless of stimulation leading to an inhibition of NFκB to the nucleus.

These results are consistent with what is known about these pathways and their activation of inflammatory factors. Results of treatment with TAKinib were consistent with the hypothesis that TAK1 is playing a key role in these pathways. Because we did not look specifically at TAK1 and pTAK1 levels, we cannot determine if TAK1 is being phosphorylated or completely inhibited. While inhibitors have been shown to cross react with other kinases, TAKinib has been shown to be specific to TAK1. However, studies need to be done to determine if this is the case.

TAKinib works as an inhibitor of TAK1 by binding to the ATP-binding pocket of TAK1. This binding inhibits TAK1's "substrate-like" autophosphorylation [58]. This inhibition slows down the step of TAK1 activation. TAKinib has also been shown to be highly specific to TAK1 and does not interfere with any of the MAP2Ks or MAP3Ks pathways or p38. This study characterizing TAKinib also found that this inhibitor induces apoptosis following TNFα stimulation in breast cancer and rheumatoid arthritis in vitro [58].

Approaching these questions in vivo, with pure microglial cultures, allows us to determine if TAK1 can be activated in microglia specifically. These preliminary studies help lay the groundwork for the role of TAK1 in microglia which can be further studied in vivo. Studies of TAK1 in vivo can be complicated given that TAK1 is present in a variety of organs and has been found to help regulate cell death, cell survival, and cell proliferation. TAK1 acta a molecular hub, downstream and upstream of various pathways that converge at TAK1.

2.5.3 Pericyte loss is occurring in STZ-treated animals

The in vitro studies suggest that TAK1 is involved in inflammatory responses in microglia. We then wanted to test the role of TAK1 in inflammation in vivo. DR is a disease affecting millions of people due to diabetes that is well documented to have chronic levels of inflammation in its progression. Previous work in the lab has shown that DR has an increase in inflammation in 2 animal models of the disease early on. In order to test TAK1 in inflammation in this disease, it would be more advantageous to use an animal model of diabetes that is inducible. STZ injections allow for chemical induction of a diabetic phenotype. STZ is a drug that was administered intraperitoneally that works by killing off the beta cells of the pancreas to mimic a type 1 diabetic phenotype and in adult mice, also results in an inflammatory response. Type 1 diabetes has been linked to chronic inflammation [87]. Three key players that have been linked to this chronic inflammation in type 1 diabetes include IFNγ, TNFα, and IL1-beta [88]. Loss of beta cells and increased insulin levels contribute to chronic inflammation and impacts the progression of DR and this inflammation may be the cause of pericyte loss seen in early stages of DR.

In order to test TAK1 in inflammation in a conditional knockout, it is essential to determine when the neurovascular unit would be affected in this same animal model. Determining the timepoint in which pericytes are lost is important in order to be able to replicate in conditional TAK1 knockouts. C57BL/6 mice were treated with vehicle or STZ and their blood glucose monitored. STZ treated animals maintained a blood glucose reading of 250mg/dL or above, whereas their WT littermates maintained a blood glucose reading below that threshold for their respective age groups. Animals were allowed to reach 4, 6, and 10 weeks post injections before being sacrificed. Retinas were

dissected out and immunolabeling was done on them to label for NG2, a marker for pericytes. As previously mentioned, STZ treated mice showed a decreased quantity of pericytes at 6 and 10 weeks compared to 4 weeks while there remains no statistical change between vehicle treated animals in those time groups. In STZ treated mice, there was a decrease in pericyte number from 4 week STZ treated animals to 6 week STZ treated animals, although not statistically significant. These results differ from previous work done in the lab on DB and Akita mice that found that pericytes are being lost as early as 3 weeks. In the C57BL background, STZ-treated mice showed a statistically different number of pericytes, a measure of NVU effects, at 6 weeks and 50% drop in pericyte number at 10 weeks. Statistical analysis also shows that there is an age effect in vehicle and STZ treated mice in pericyte quantification. While there is a difference in this timepoint in which pericytes are lost, these are two different models of diabetes and have different mechanisms at play. When comparing vehicle treated animals, there is a decreasing trend in pericyte numbers. The same is apparent in the STZ treated animals, there is a decreasing number of pericytes as the age of the STZ animals increase. This suggests that there may be variability between animals and that pericytes may be naturally decreasing to a certain extent in mouse retina. This is important to consider moving forward. Pericytes are incredibly important to the integrity of the BRB and are essential for stabilization. In animals 6 and 10 week time points, there also appeared to be vascular changes such as microaneurysms and branching, although this was not quantified.

2.5.4 Future directions

IFNγ has been shown to activate NFκB through the PERK pathway but has not been previously linked to acting through the TAK1 pathway to activate NFκB. While this preliminary data shows that inhibiting TAK1 using TAKinib inhibits the activation of NFκB, studies need to be done to further explore the relationship between IFNγ and TAK1. Increasing the number of experimental replicates along with western blots and inflammatory panels can help elucidate the relationship between IFNγ and TAK1 signaling. Other growth factors such as BMP7 and IL-1beta have also been shown to work through the TAK1 pathway in heart disease and cancer and warrant further exploration in regards to inflammation and DR [89]. TNFα and LPS on the other hand has been shown to recruit the TAB1/TAK1 complex leading to NFκB activation [82]. Both have also been

shown to increase ROS production and cell apoptosis in murine macrophages [90]. Our results support what the literature suggests.

In-vitro studies may not have the same effect in vivo. In order to apply our in vitro studies to in vivo, we first had to determine timepoints pericytes are being lost in an STZ type 1 diabetic mouse model. Retinal flatmounts of mice treated with STZ showed a decrease in pericytes starting at 6 weeks post injection. It is possible that pericyte loss is happening earlier on; this study was done on a smaller number of experimental replicates and should be increased. Studying TAK1 further is necessary to better understand the mechanisms in which it is working within microglia. We need to look at pTAK1 compared to total TAK1 in these treatments. We attempted to do this but encountered issues with TAK1 and pTAK1 antibodies which, with time, can be trouble-shot. Future studies also would include treating microglia cells with an AGE ligand which I mentioned earlier is not commercially available and can pose issues when attempting to create in a lab given the length of time needed to create. It is also important to look at levels of JNK and p38 relative to their phosphorylated forms when treated with activators and in or without the presence of TAKinib to see if TAK1 specific labeling is affected.

Inflammatory panels using multiplex ELISA and qPCR to determine the effects of the ligands with and without the inhibitors will allow us to further explore what is happening in microglia in regards to secreted factors.

Determining that IFNγ, TNFα, and LPS activate downstream factors of TAK1 and this response can be inhibited using TAKinib, confirms that pro-inflammatory factors trigger activation of TAK1 in microglia. Combined with seeing a loss of pericytes in an STZ diabetic model at 6 weeks allows us to determine a timepoint to create an inducible TAK1 knockout specific to microglia. The goal is to create an inducible knockout of TAK1 in microglia and then treat these knockout animals with STZ to induce a type 1 diabetic phenotype. Analysis of these animals will give a better idea the type of role TAK1 is playing in microglia in the progression of DR. Knockout of TAK1 in microglia may result in inhibition of inflammation. Whether this inhibition is partial or whole will have to be determined. Microglial specific deletion of TAK1 has been shown to result in neuroprotective effects in ischemic stroke [61]. In order to determine if inhibiting TAK1 in this

conditional knockout increases the health of the NVU, STZ treatment done in these studies will be replicated in those animals at 6 and 10 weeks post STZ treatment, the timepoint at which we found a statistical decrease in pericyte numbers. Based on these previous studies and our timeline of STZ effects on pericyte loss obtained here, transgenic animals will be treated with STZ to create a diabetic phenotype and animals will be sacrificed at 10 weeks and retinal tissue taken for analysis. Retinal flatmounts with labeling for pericytes using NG2 will give an initial indication as to whether pericyte number has decreased from wildtype animals. If our hypothesis holds true and TAK1 is working through microglia to create an inflammatory response that affects the NVU in DR, inhibition, or knockout of TAK1 in microglia would potentially increase the health or inhibit damage to the NVU.

CHAPTER 3. TAK1 IN CHICK RETINAL DEVELOPMENT

3.1 Abstract

Coordination of the cell cycle with proliferation and differentiation is essential to obtain the right number of cells at the appropriate time during the development of the central nervous system. Cell cycle length, in particular that of the G1 phase of the cycle, has been coupled to differentiation in the central nervous system, but the mechanism as well as the reason behind an increase in the length of the cell cycle are unclear. Previous studies have proposed that the length of the G1 phase is a critical determinant in the accumulation of differentiation factors in progenitor cells. The cell has a better chance of amassing factor(s) necessary for the differentiation process with a longer cell cycle. The studies herein focus on a potential role for transforming growth factor β-activated kinase 1 (TAK1), a hub kinase that lies at the intersection of multiple signaling pathways, in the coordination of cell cycle exit and differentiation in the chick retina. Previous studies have focused predominantly on the role this kinase plays in the inflammation process and axonal growth. TAK1 is downstream of multiple signaling pathways that are critical to development of the central nervous system, including transforming growth factor β (TGFβ), bone morphogenetic proteins (BMPs), and WNTs. The present study indicates that activated TAK1 is found throughout the developing chick retina; however, it is localized at higher levels in dividing and differentiating cells. Further, chick *ex ovo* retinal studies using TAK1 inhibitor 5Z-7-oxozeaenol increased both progenitor and differentiating cell populations, accompanied by a substantial increase in proliferation and a smaller increase in cell death. These results indicate that TAK1 may be involved in cell cycle progression.

3.2 Introduction

The hierarchical organization of the mature neural retina, containing seven basic cell types, is common to vertebrate retinas [91, 92]. The developing retina is comprised of homogeneous group of cells called retinal progenitors which generate groups of cell types at specific stages throughout development [93, 94]. In most animals, cell cycle length is known to increase throughout development, increasing the length of G_1 and increasing the overall time of cell division [95, 96].

Many studies have confirmed that retinal progenitors are mostly multipotent. However, progenitors change in their capacity to generate earlier born cells at later stages of development [91, 97, 98]. Differentiation of retinal cell types is the result of signaling pathways and transcription factors activity which regulate cell type specification [97, 99-101]. Likewise, the activation of specific signaling pathways and cell cycle genes is essential for cells that remain in the cell cycle. Many of the key questions that still remain, lie in the regulation and coordination of cell cycle exit and differentiation, and the responsible signaling pathways that govern the process.

When cell cycle exit does not function properly, issues such as hyperplasia and lack of differentiated cell types lead to improper function of the retina [102]. Across various species, multiple factors have been identified that play a role in cell cycle exit, including extrinsic factors, signaling pathway members, and transcription factors [102, 103]. In addition to this, there are factors that are associated with shortening of the cell cycle such as transcription factor *E2f1*, cyclin G2 [95] and factors associated with the lengthening of the cell cycle such as *Erf* and *Fbxw7* [95]. Transforming growth factors β (TGFβs), sonic hedgehog (SHH), and bone morphogenetic proteins (BMPs) are all secreted factors that have been implicated in cell cycle regulation, all of which have been implicated in both proliferation and cell cycle exit [104-107].

Many transcription factors that either drive cells to exit the cell cycle and/or drive cell type-specific differentiation have been implicated as well [108-111]. Cyclin-dependent kinase inhibitors p27 and p57 are signaling proteins which are necessary for inhibiting the retinoblastoma protein necessary to control cell cycle exit and these cyclins have also been implicated in cell cycle length [112]. When it comes to cell cycle exit, there is evidence to suggest that in retinal development it is more complex than previously shown, which indicates that there may be influential signaling factors yet to be evaluated [103].

Transforming growth factor β-activated kinase 1 (TAK1) is a serine-threonine kinase that is regulated by multiple signaling pathways, including tumor necrosis factor α (TNFα), interleukin 1 (IL1), toll-like receptors (TLRs), TGFβ, and BMPs [82, 113-115]. TAK1 acts as a hub kinase that combines extracellular signaling events and concentrates those signals on the regulation of mitogen activated kinase kinase 3/6 (MKK3/6), MKK4/7, and IκB kinase (IKK). It has been

determined that MKK3/6 regulates p38, MKK4/7 activates c-jun N-terminal kinase (JNK), and phosphorylation of IKK leads to the destruction of IκB, allowing NFκB to be transported to the nucleus [116]. JNK and its upstream regulators MKK4/7 are key regulators of retinal ganglion cell death in vertebrates [116, 117]. A recent study in retinal development showed that a loss of both MKK4 and MKK7 led to a decrease in JNK signaling and a subsequent decrease in retinal ganglion cells [118]. While the role of JNK, MKK4 and MKK7 have been investigated, the role of TAK1 in retinal development is yet to be discovered.

The study described here investigates the role of TAK1 in chick retinal development. Using immunofluorescence, we describe localization patterns of activated phospho-TAK1 (pTAK1) at critical stages of retinal development from the optic cup up to embryonic day 18 (E18). With further analysis, we investigated a potential role for pTAK1 in E6 retina by treating *ex ovo* retinal cultures with a TAK1 inhibitor. The results of this study have led us to hypothesize that TAK1 is responsible for increasing cell cycle length.

3.3 Materials and methods

Tissue collection and processing

Fertilized white leghorn chicken eggs were procured from University of Michigan and stored at 16°C in a BOD (Biological Oxygen Demand) incubator (Jeio tech: IL-11A). Eggs were incubated at 37ºC for the specified periods of time (Kuhl, Flemington, NJ). Eyes were enucleated and extraocular tissues removed in 1X phosphate buffered saline (PBS) and fixed overnight in 4% paraformaldehyde diluted in 0.1M phosphate buffer, pH7.4. Samples were rinsed twice in 1X PBS at room temperature incubated overnight with increasing concentrations of sucrose solutions in order: 5%, 10%, 15%, and 20% sucrose made in 0.1M phosphate buffer, pH 7.4. Samples were then placed in 20% sucrose and optimal cutting temperature (OCT) medium at a ratio of 3:1 (4583 Tissue-Tek, Sakura, Torrance CA). The samples were incubated in the 3:1 solution and oriented so that sections would be taken through the naso-temporal axis. They were then placed in dry ice to freeze and stored for future sectioning at -80°C. Samples were sectioned using a Leica CM3050 S cryostat at a thickness of 12µm and placed on vectabond-coated (Vector Labs, Burlingame, CA) superfrost plus slides (Fisher Scientific, Pittsburgh, PA) and then stored at -80ºC.

Immunohistochemistry

Slides with cryosections previously stored at -80°C were thawed to room temperature (RT) and the perimeter of the sections was lined using a peroxidase anti-peroxidase (PAP) pen (Electron Microscope Sciences, Hatfield, PA, Cat #71310). All immunohistochemistry steps were conducted at RT in a humid chamber lined with wet filter papers covered by nylon mesh unless otherwise noted. Tissue samples were fixed with 4% paraformaldehyde made in 0.1M phosphate at pH7.4 for 30 minutes and then rinsed twice with 1X PBS for two minutes. Sections were permeabilized with methanol for 10 minutes and subsequently rinsed with 1X PBS. Antigen retrieval was conducted by treating sections with 1% SDS in 0.01M PBS (Fisher Scientific, Pittsburgh, PA) for 5 minutes and then rinsed for 5 minutes three times with 1X PBS. Tissue was rinsed twice with 1X borate buffer at pH 8.0 for 5 minutes and then rinsed twice with 1X PBS for 5 minutes. Following these steps, sections were then treated with fresh 1% sodium borohydride (Acros, New Jersey) in 1X PBS for 2 minutes to reduce auto fluorescence. Sections were then blocked with 10% donkey or goat serum for 30 minutes. After blocking, primary antibodies were diluted into a cocktail of 0.025% triton-X diluted into 1X PBS and 2% of goat or donkey serum to their respective concentrations and added to sections. Sections were incubated with primary antibody solution overnight at 4°C. Primary antibodies that were amplified with biotin-streptavidin were used at half of their normal concentration and incubated in the same fashion. After overnight incubation with primary, samples were rinsed using 1X PBS twice before being treated with secondary antibody or a biotinylated antibody. Secondary antibodies were diluted with 1X PBS at their respected concentrations and placed on slides incubated at room temperature for 1 hour in the dark. Subsequently, sections were rinsed with 1X PBS twice for 2 minutes before being incubated with 2µg/ml Hoechst stain (Invitrogen, Cat #H1399) for two minutes. For samples subjected to biotin amplification, samples were treated with DyLight conjugated streptavidin (DyLight 549, Vector Labs, Burlingame, CA, Cat# SA-5549-1) for an additional hour followed by a rinse with 1X PBS and incubation for 2 minutes with Hoechst. Finally, sections were rinsed twice more with 1X PBS and then prepared with mounting medium aqua polymount (Polyscience Inc, Warrington, PA, Ca#18606-20) and cover slipped (Electron Microscopy Sciences, Hatfield, PA, Cat #71310), the edges of which were sealed with clear nail paint (Electron Microscopy Sciences, Hatfield, PA, Cat #71310).

For co-labels with antibodies against phospho TAK1 (pTAK1) and other antibodies raised in rabbit, citrate antigen retrieval with tyramide amplification was done following permeabilization with methanol. Briefly, sections were incubated with 10mM sodium citrate with 0.05% Tween pH 6.0 for 1 hour at 63ºC, then allowed to cool for 20 minutes followed by two rinses of with 1X PBS. Sections were subsequently treated for 2 minutes with 1% sodium borohydride (Acros, New Jersey) in 1X PBS and then blocked with 10% donkey or goat serum in 1X PBS containing 0.25% Triton X-100 for 30 minutes. Primary antibodies were then diluted 5 to 10 times normal concentration in a solution of 2% donkey or goat serum and 0.025% triton X-100 diluted in 1X PBS. After incubation overnight at 4ºC, sections were rinsed with 1X PBS and incubated with 3% solution of hydrogen peroxide in methanol for 15 minutes. Sections were washed with 1X PBS twice for 2 minutes before being incubated with biotinylated secondary antibody (Vector Labs, Burlingame, CA) in 1X PBS in the dark for one hour at room temperature. Sections were then washed using HRP streptavidin (Vector Labs, Burlingame, CA) in 1X PBS 1:1000 (and 1:500 for pSMAD1) for an hour in the dark. Afterwards, slides were then washed twice in 0.1M Tris-HCl, 0.15M NaCl, 0.05% Tween-20 (TNT) buffer and incubated with fluorescein plus amplification reagent diluted 1:300 in 1X tyramide signal amplification (TSA) amplification diluent (Perkin Elmer, Waltham, MA, Cat# NEL741001KT) for 5 min in the dark. Slides were subsequently washed twice in TNT buffer followed by two, 2-minutes rinses in 1X PBS, counterstained with hoechst solution and mounted with aqua polymount and cover slipped. All images were acquired using an Olympus Fluoview FV 1000 confocal microscope.

Table 3.1 Antibodies used in study

Antigen	Source	Antibody Dilution	RRID Number
Phospho-TAK1 (Cat # ab79583)	Abcam (Cambridge MA)	1:100	AB_1659038
Phospho-TAK1 (cat# ab192443)	Abcam (Cambridge, MA)	1:100	AB_2819208
Phospho-histone 3 (Cat # 9706)	Cell Signaling (Danvers, MA)	1:800	AB_331748
AP2α (3B5)	Developmental Studies Hybridoma Bank (Iowa City, IA)	1:30	AB_528084
BRN3A (Clone5A3.2)	Millipore	1:100	AB_92154
SOX2 (Cat# sc17320)	Santa Cruz (Santa Cruz, CA)	1:250	AB_2286684
Visinin (7G4)	Developmental Studies Hybridoma Bank (Iowa City, IA)	1:30	AB_528510
Islet1 (39.4D5)	Developmental Studies Hybridoma Bank (Iowa City, IA)	1:30	AB_2314683
NAPA73 (E/C8)	Developmental Studies Hybridoma Bank (Iowa City, IA)	1:20	AB_531792
Phospho-JNK	Millipore	1:300	AB_310412
Cleaved caspase 3 (cat#9661)	Cell Signaling (Danvers, MA)	1:300	AB_2341188
β-tubulin (Cat# T0198)	SIGMA (St. Louis, MO)	N/A	AB_477556

Western Blots

Chick retinas were dissected out and placed in lysis buffer (5M NaCl, 1M Tris, 0.5M EDTA, 5% TritonX-100 at pH 8.0 with 4% protease inhibitor cocktail and 1% phenylmethylsulfonyl fluoride (PMSF; Sigma) (Cas # 329-98-6) for 20 minutes on ice. Tissue lysates were then centrifuged at 14,000 rpm for 15 minutes at 4ºC and the supernatant was collected for protein estimation using bicinchoninic acid (BCA) assay (Thermofisher Scientific, Rockford, IL) (Cat # 23225). Fifty µg of total protein were combined with loading dye at a 1:3 ratio. This was then loaded onto a 10% SDS polyacrylamide gel (Nalgene) and then run for an hour at 150 volts. Proteins were transferred from gel to Polyvinylidene fluoride (PVDF) membrane (Bio-Rad laboratories, Inc. Hercules, CA) (Cat #1620174) at 4ºC at 100 volts for 60 minutes in transfer buffer. Membrane was blocked using Pierce protein-free T-20 (TBS) blocking buffer (Thermofisher Scientific, Rockford, IL) (Cat #37571) for 30 minutes and incubated overnight at 4ºC with β Tubulin antibody at 1:10,000 on day 1 as our endogenous control. On day 2, the membranes were washed with 1X TBST twice and subsequently incubated with a peroxidase conjugated secondary antibody (1:5000 goat anti-rabbit HRP in 1X TBST) (Invitrogen Cat #31460) at room temperature for one hour in the dark. The membranes were then treated with SuperSignal West Femto Chemiliminescent Substrate (Thermofisher Scientific, Rockford, IL) (Cat # 34095) for two minutes and was covered in saran wrap and stored in a light protective cassette. The blot was visualized using x-ray files (Thermoscientific, Rockford, IL).

Ex Ovo Cultures/whole retinal explants

Method for retinal explants was adapted from [119]. Briefly, extraocular tissue was removed from enucleated eyes and eyes subsequently incubated in 37ºC 1X PBS to get to aid in removal of pigmented epithelium with sharpened Dumont forceps. Explants were transferred into a well containing 1mL culture medium. Culture medium was prepared using 10% FBS, 2mM Glutamax™, 10u/mL penicillin streptomycin, 5 µg/ml Insulin, and 1:1 DMEM : F12 Nutrient mix (Thermofisher Scientific, Rickford, IL) (Cat # 10565018). Each retinal explant was incubated in a single well of a 24 well plate at 37ºC for 1 hour on a rotator shaker inside a cell incubator with 5% CO_2 at 50 RPM. Following this, retinal explants were either treated with vehicle (DMSO) as a control, or with 2 mM of the TAK1-specific inhibitor, (5Z)-7-Oxozeaenol (Tocris) (Cat #3604). Following treatment with vehicle or inhibitor, retinal explants were incubated at 37°C on a shaker

with 5% CO_2 at a speed of 50 RPM for 24 hours. Subsequently, the 24 well plate containing the explants was removed from the incubator, retinal transplants were transferred into a new 24-well plate containing 4% paraformaldehyde in 1X PBS and incubated on ice for 15 minutes. Afterwards, retinal transplants were rinsed with 1X PBS for 10 minutes in the 24 well plate on ice. Whole retinal explants were transferred to wells with increasing concentrations of sucrose: 5%, 10%, 15%, and 20% sucrose in 1X PBS, incubating on ice for an hour if the chick embryo was E3 or younger and an addition 1-2 hours if older than E3. Retinal explants were then placed into 3:1 OCT: sucrose solution and into an embedding mold. Embedded retinal explants were flash frozen on dry ice until frozen solid. Samples were stored at –80°C until ready to be sectioned.

3.4 Results

Phosphorylated TAK1 (pTAK1) is heavily expressed in dividing and differentiating cells of the developing chick retina and lightly in non-dividing progenitors

To examine the localization of TAK1 in the developing chick retina, immunohistochemistry was performed on sections from embryos at embryonic day 3 (E3), E5, E8, E15, and E18. E3 is representative of the stages when the retina is populated primarily with proliferative progenitors. E5 is representative of stages when early retinal cell types, such as cone photoreceptors and retinal ganglion cells are present, in addition to proliferative progenitors. E8 is a mid-developmental stage when most cell types have been generated in the retinal fundus and distinct outer and inner plexiform layers are beginning to form. By E15, there is a fully laminated retina; however, cells are still differentiating and refining connections. By E18, a mature retina is present, although there is evidence that some cell types continue to develop [120].

Retinal cryosections were labeled using an antibody that recognizes activated TAK1, phosphorylated at threonine 184/187 (pTAK1) coupled with a Hoechst label to visualize nuclei in the tissue. At E3, pTAK1 heavily labeled dividing cells at the scleral edge of the retina and weakly labeled retinal pigmented epithelium (RPE), retinal neuroblasts, and lens (Figure 3.1A-C).

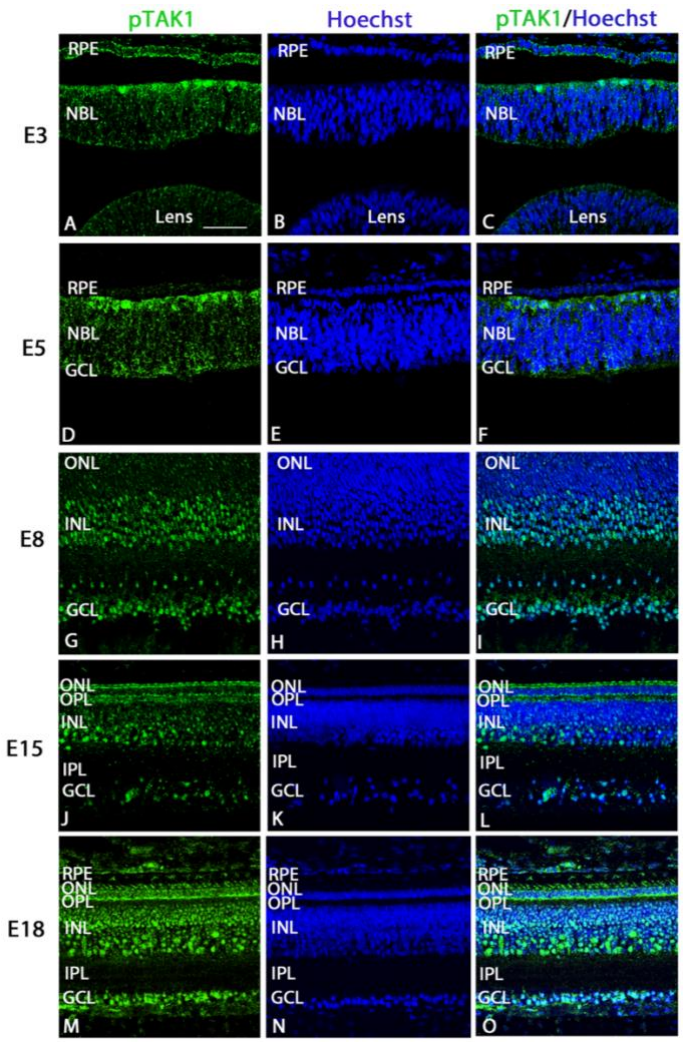

Figure 3.1 Phosphorylated TAK1 (pTAK1) weakly labels progenitor cells and heavily labels dividing and differentiating cells of the developing retina. Retinal sections from E3, E5, E8, E15, and E18 chick embryos were co-labeled for pTAK1 (A, D, G, J, M, P) and Hoechst nuclear stain (B, E, H, K, N, Q). Overlap in labels is shown in C, F, I, L, O, R. Abbreviations: RPE, retinal pigmented epithelium; NBL, neuroblast layer; INL, inner nuclear layer; GCL, ganglion cell layer; OPL, outer plexiform layer; IPL, inner plexiform layer. Scale bar in A=50μm for images A-R

The RPE and cells of the retinal neuroblast layer (NBL) continued to be weakly labeled at E5 (Figure 3.1D-F); however, cells at the vitreal edge of the retina in the presumptive ganglion cell layer (GCL) appeared to be more strongly labeled (Figure 3.1D-F). Dividing cells at the scleral edge were still strongly labeled for pTAK1 (Figure 3.1D-F). At E8, the GCL and inner part of the inner nuclear layer (INL), where presumptive amacrine cells would be found, were strongly

immunolabeled for pTAK1, whereas the cells of the outer nuclear layer and outer portion of the INL were either negative or weakly labeled (Figure 3.1G-I). Immunolabel at E15 appeared to be widespread in the retina, with strong signal present in the inner part INL, GCL, and outer plexiform layer (OPL), while weaker label was present in the remaining retina (Figure 3.1J-L). Label in the ONL was restricted primarily to the inner segment (Figure 3.1J-L). Finally, at E18, pTAK1 appeared to be localized throughout the retina, with similar patterns and strengths as those found at E15 (Figure 3.1M-O). In addition to the photoreceptor inner segments, signal also appeared to be present in the outer segment region (Figure 3.1M-O). Retinal localization patterns were confirmed by performing immunofluorescence using a second antibody that also recognizes pTAK1 (T184, 187) at E8 (Figure 3.2).

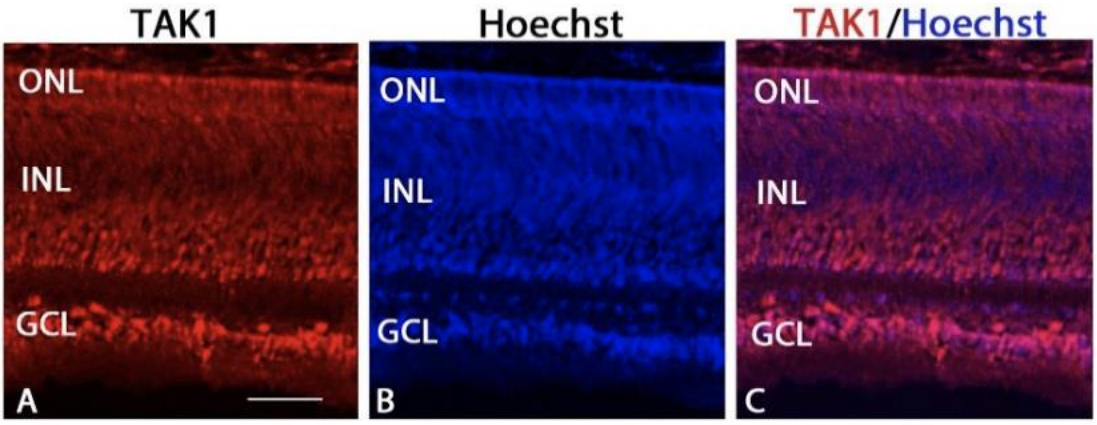

Figure 3.2 Confirmation of TAK1 immunolabeling at E8. Retinal sections from E8 chicken embryos were labeled with a Hoechst (nuclei) and a second pTAK1-specific antibody (BIOSS). As was seen in Figure 1, pTAK1 was detected throughout the retina, with stronger label appearing in the outer nuclear layer (ONL), the outer half of the inner nuclear layer, and the ganglion cell layer (GCL). Scale bar in A =50μm for images A-C.

Sections from each stage treated with isotype specific IgG in place of the primary antibody showed weak background label at the scleral edge of the retina at E5, E12-18 and weak label in the outer plexiform label at E12. Otherwise, the retina was negative for any immunofluorescence (Figure 3.3A). Retinal lysates from E5, E8, E15 and E18 embryos were analyzed for pTAK1 expression by western blot (Figure 3.3B). At each stage, a single band was detected at a molecular weight of

approximately 68kDa. Specificity of the pTAK1 antibody was tested by neutralizing antibody with the immunizing peptide. Weak, non-specific label was detected primarily at the scleral edge of the retina from E3-E12, and in the outer plexiform layer at E15 and E18 (Figure 3.4).

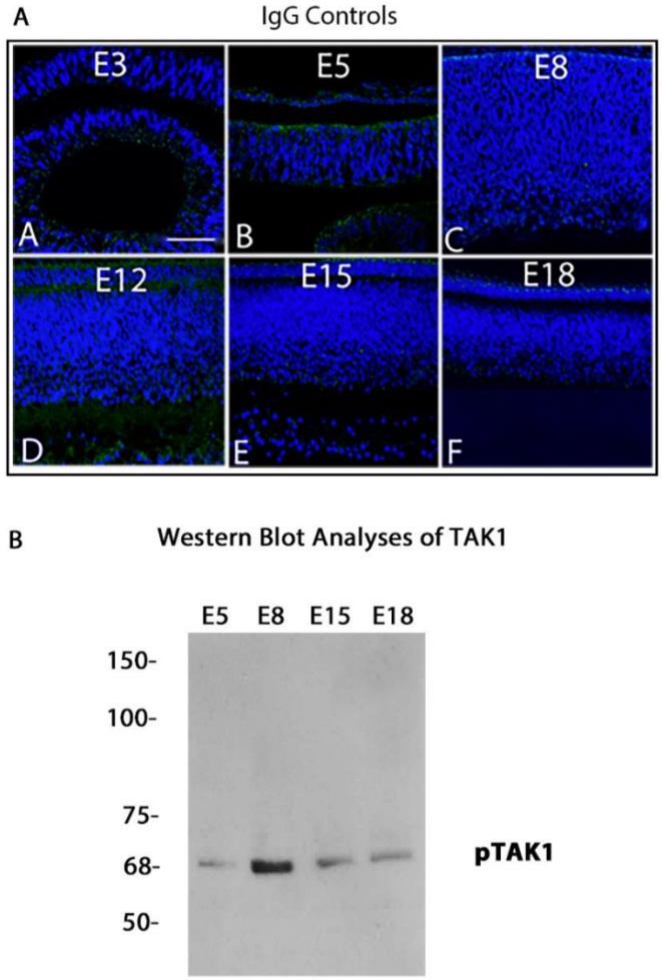

Figure 3.3 IgG controls for pTAK1 immunofluorescence and immunoblots for pTAK1. A) Retinal sections from E3, E5, E8, E12, E15, and E18 chick embryos were incubated with isotype specific IgG in place of the primary antibody and incubated with secondary as usual. B) Immunoblot of lysates from E5, E8, E15 and E18 retina showed a single band at 68kDa. Lower insert shows β-tubulin loading control. Scale bars in A, A = 50μm for images A-F.

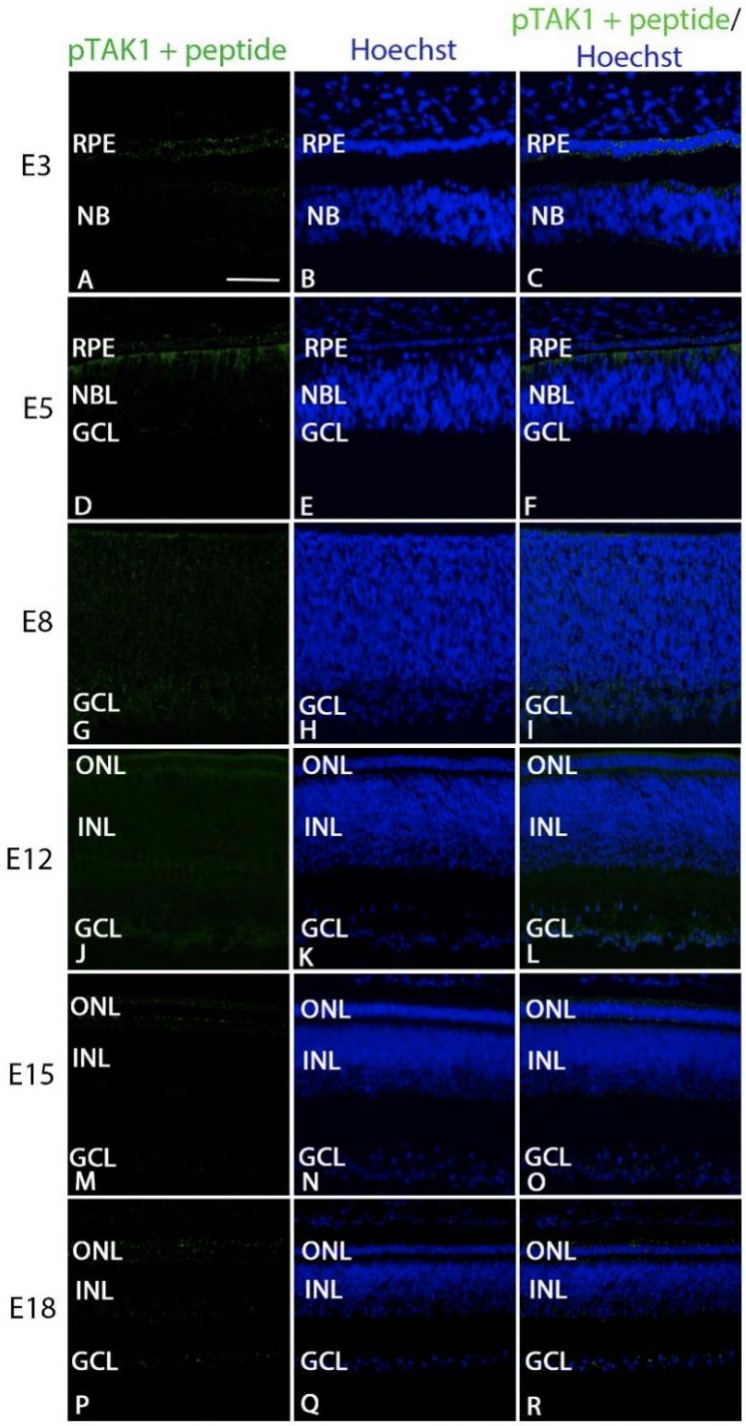

Figure 3.4 Immunolabel with pTAK1 preabsorbed with immunizing peptide. Retinal sections from E3, E5, E8, E12, E15, and E18 chick embryos were co-labeled pTAK1 (A,D, G, J, M, P) and Hoechst nuclear stain (B, E, H, K, N, O). Overlap in labels is shown in C, F, I, L, O, R. Abbreviations: RPE, retinal pigmented epithelium; NBL, neuroblast layer; INL, inner nuclear layer; GCL, ganglion cell layer. Scale bar in A= 50μmfor images A-R.

pTAK1 labeled dividing cells strongly and retinal progenitors weakly

Examination of immunolabel in Figure 1 suggested that pTAK1 was heavily localized to dividing retinal progenitor cells and lightly to non-dividing progenitors. To confirm pTAK1 localization in both progenitor populations, double-label fluorescence was carried out. Sections from E3, E5, and E7 double-labeled for phospho-histone 3 (pH3), a marker of prophase in proliferating cells, and pTAK1 were analyzed for co-label (Figure 3.5A-I). At each stage examined, $pH3^{+}$ cells all appeared to be co-labeled with pTAK1. To determine if pTAK1 was also present in retinal progenitors not actively dividing, sections from E3, E5, E8 and E18 embryos were double-labeled for SRY (sex determining region Y) - box 2 (SOX2) and pTAK1. At early stages (E3 and E5), SOX2 labels all retinal progenitors, while in later stages (E8 and E18) SOX2 labels Müller glial cells, astrocytes, and cholinergic amacrine cells. E3 and E5 retinal sections co-labeled with SOX2 showed a high degree of overlap with pTAK1 (Figure 3.5 A-I). At later stages of the retina development, E8 and E18, SOX2 labeled cholinergic amacrine cells (Figure 3.6J-L, arrowheads), Müller glia (Figure 3.6J-L, open arrows) and retinal astrocytes (Figure 3.6J-L, closed arrows).

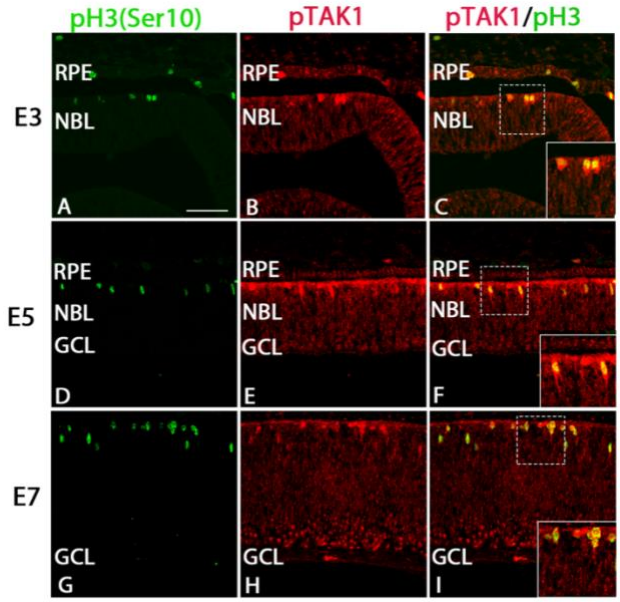

Figure 3.5 pTAK1 was co-localized to the phospho-histone 3+ (pH3+) dividing cells of the early chick retina. Chick retinal sections from E3, E5, and E7 embryos were double labeled with pH3 (A, D, G) and pTAK1 (B, E, H). Co-label is shown in C, F, and I. Dashed boxes in C, F, and I are shown at higher magnification in insets in C, F, and I. Abbreviations: RPE, retinal pigmented epithelium; NBL, neuroblast layer; GCL, ganglion cell layer. Scale bar in A = 50μm for images A-I.

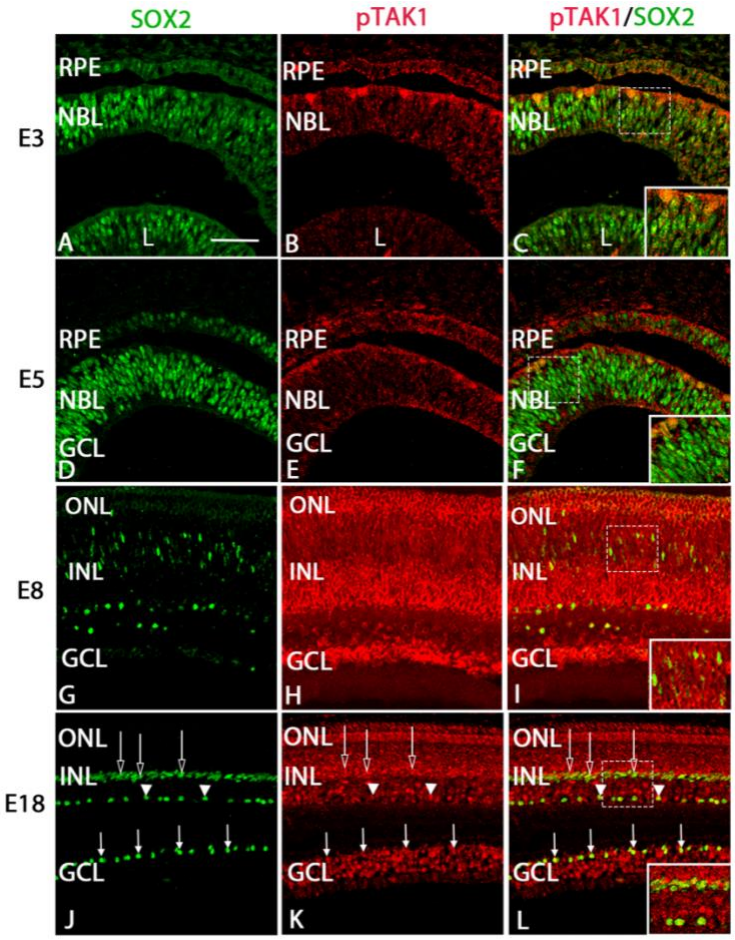

Figure 3.6 pTAK1 was co-localized to SOX2^{+} retinal progenitors in the early chick retina and a subset of Müller glial, cholinergic amacrine, and astrocyte cells in later stages. Chick retinal sections from E3, E5, E7, and E18 embryos were double-labeled with SOX2 (A, D, G, J) and pTAK1 (B, E, H, K). Co-label is shown in C, F, I, and L. Open arrows indicated Müller glia, closed arrows indicate retinal astrocytes, and arrowheads indicate cholinergic amacrine cells (J, K, and L). Dashed boxes in C, F, I, and L are shown at higher magnification in insets in C, F, I and L. Abbreviations: RPE, retinal pigmented epithelium; NBL, neuroblast layer; INL, inner nuclear layer; GCL, ganglion cell layer. Scale bar in A = 50μm for images A-L.

pTAK1 was localized to populations of cells expressing cell type-specific markers at E8 and E18.

To determine which populations of differentiated cells pTAK1 might be found in, we analyzed sections from E8 and E18 double-labeled for pTAK1 and cell type-specific markers such as SOX2 (cholinergic amacrine, Müller glia, and astrocyte cells), LIM1/2 (horizontal cells), CHX10 (bipolar cells), AP2α (amacrine), and BRN3A (ganglion cells). At E8, TAK1 was co-localized with cells

positive for SOX2, LIM1/2, CHX10, AP2α, and BRN3A (Figure 3.6G-I and Figure 3.7). A subpopulation of cells labeled with Visinin appeared to be co-labeled with TAK1 (Figure 3.7A-C). TAK1 also co-localized with cells expressing SOX2, LIM1/2, CHX10, AP2α, and BRN3A at E18 (Figure 3.6J-L and Figure 3.8D-O). TAK1 also heavily labeled inner and outer segment regions and the synaptic region of Visinin^{+} photoreceptors at E18 and weakly labeled photoreceptor cell bodies (Figure 3.8A-C).

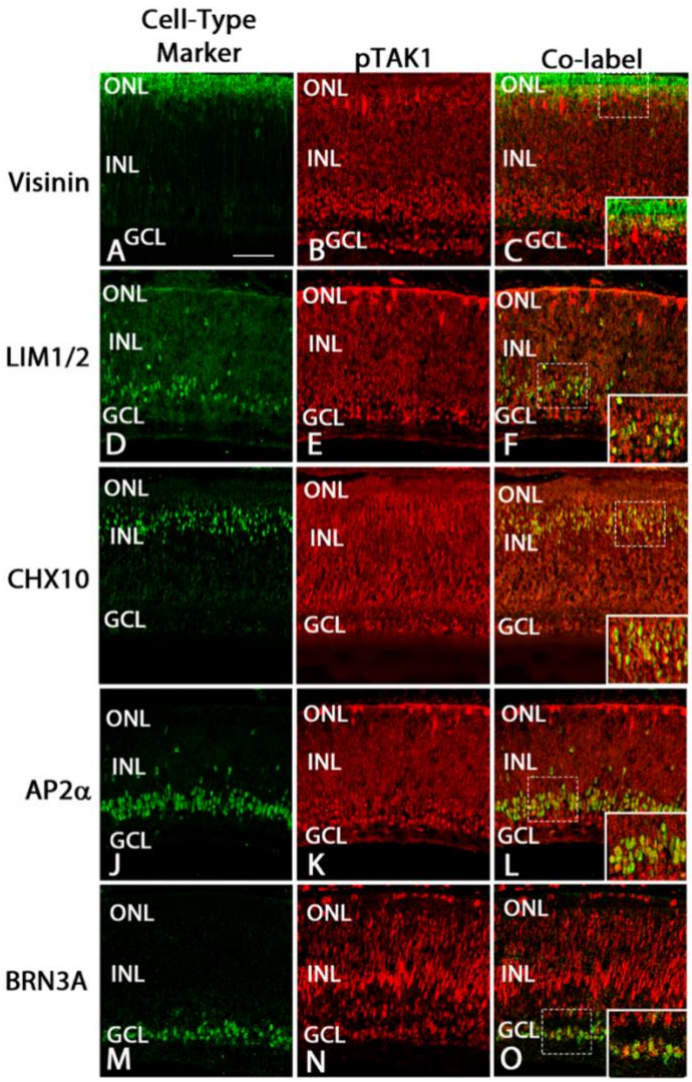

Figure 3.7 pTAK1 was localized to differentiating cells in E8 retina. Chick retinal sections from E8 embryos were double-labeled with pTAK1 and Visinin (cones; A-C), LIM1/2 (horizontal cels; D-F), CHX10 (bipolar cells; G-I), AP2α (amacrine cells; J-L) or BRN3A (ganglion cells; M-O). Dashed boxes in C, F, I, L, and O are shown at higher magnification in insets in C, F, I, L, and O. Abbreviations: ONL, outer nuclear layer; NBL, neuroblast layer; INL, inner nuclear layer; GCL, ganglion cell layer. Scale bar in A = 50μm for images A-O.

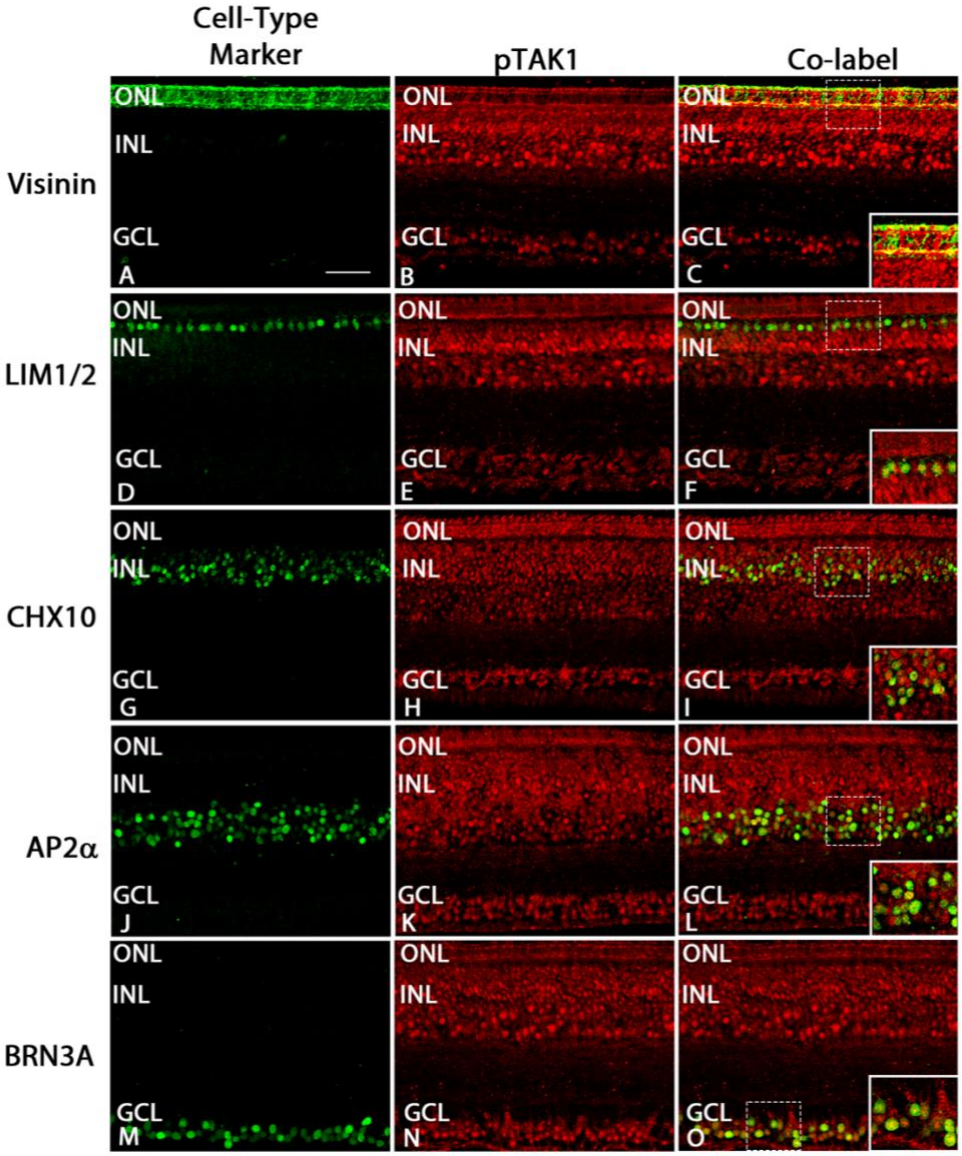

Figure 3.8 pTAK1 was localized to differentiated cells at E18. Chick retinal sections from E18 embryos were double-labeled with pTAK1 and Visinin (photoreceptors; A-C), LIM1/2 (horizontal cells; D-F), CHX10 (bipolar cells; G-I), AP2α (amacrine cells; J-L), or BRN3A (ganglion cells; M-O). Areas shown by dashed boxes in C, F, I, L, and O are enlarged and shown in insets in C, F, I, L, and O. Abbreviations: ONL, outer layer; INL, inner nuclear layer; GCL, ganglion cell layer. Scale bar in A = 50μm for images A-O

Retinas treated with TAK1 inhibitor (TAKi) in ex ovo cultures show reduced number of phospho-JNK labeled cells (pJNK) and an increased number labeled with cleaved Caspase 3

To examine the potential role of TAK1 in the differentiation of retinal cells, ex-ovo cultures of E6 retinas were treated with TAK1 inhibitor (TAKi), 5Z-7-oxozeaenol. Biochemically, 5Z-7-oxozeaenol forms a covalent bond with TAK1 and inhibits the kinase activity as well as the ATPase activity [9]. Initially, we determined whether the inhibitor was capable of reducing the phosphorylated and activated downstream target, c-jun n-terminal kinase (pJNK). E6 retinas were grown for 24 hours in vehicle or TAKi, sectioned and immunolabeled for pJNK (Figure 3.9). Phospho-JNK labeled cells were widespread in vehicle-treated retinas (Figure 3.9A-C), while TAKi-treated retinas showed reduced label in comparison (Figure 3.9D-F). Quantitation of the number of pJNK-labeled cells in vehicle-treated retinas (N=3) indicated 31.3% (+/- 3.52% SD) of the cells were $pJNK^+$, whereas the percentage of $pJNK^+$ cells in TAKi-treated retinas (N=3) was 17.45% (+/-2.03% SD) (Figure 3.9G).

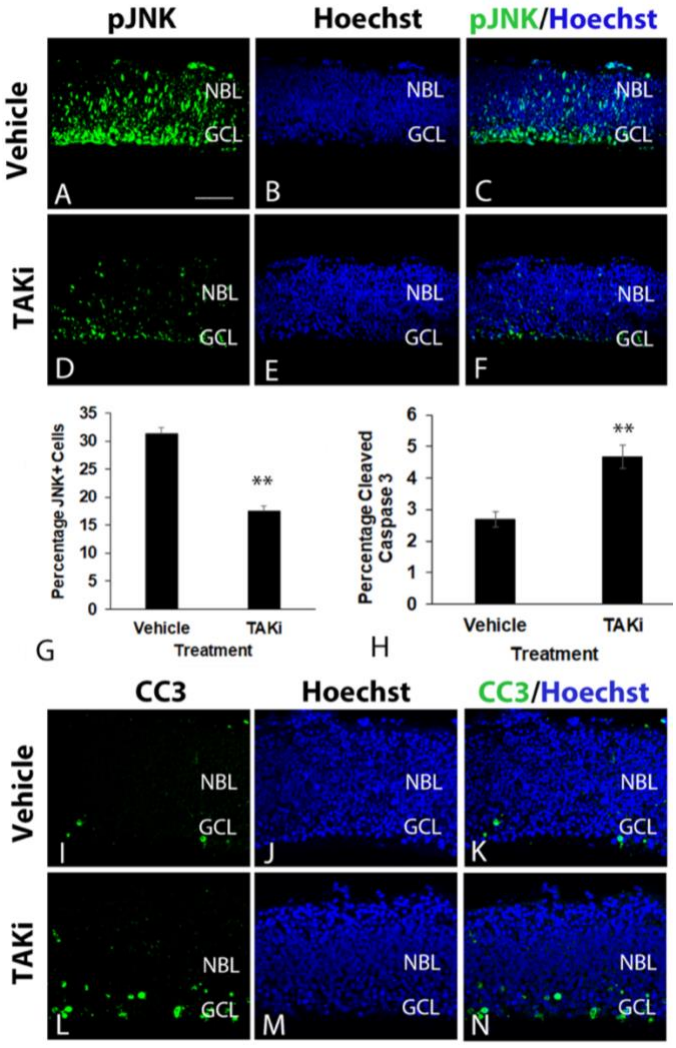

Figure 3.9 In comparison to vehicle-treated retinas, TAKi-treated retinas have a decrease in JNK labeling and an increase in cleaved-caspase 3 labeling. E6 chick retinal cultures were treated with vehicle or 2μm TAK1 inhibitor (TAKi) for 24 hours and sections through retinas were co-labeled for downstream kinase phosphor- c-jun N-terminal kinase (pJNK; A, C, D, F) or apoptosis marker cleaved caspase 3 (CC3; I, K, L, N) and Hoechst dye for DNA (blue; B, C, E, F, J, K, M, N). Percentages of labeled cells were quantified in 3 separate retinas for pJNK+ cells (G) or cleaved caspase 3 (H). Standard deviation is shown in G and H. A = 50μm for images A-F and I-N. Abbreviations: NBL, neuroblast layer; GCL, ganglion cell layer. Scale bar in A = 50μm for images A-F and I-N.

Previous investigations in some tissues have produced data showing TAK1 to be involved in cell death [1, 121, 122]. To investigate the role of TAK1 in developing retinal cell death, we examined the activation of cell death marker caspase 3 (cleaved caspase 3; CC3) in vehicle- and TAKi-

treated retinas (Figure 3.9I-N). In sections immunolabeled for CC3, there appeared to be an increase in $CC3^+$ cells in sections from TAKi-treated retinas (Figure 3.9L-N) in comparison to vehicle-treated (Figure 3.9I-K). In both vehicle- and TAKi-treated retinas, $CC3^+$ cells appeared to be localized to the GCL. Quantitation of sections through retinas (N=3 for each treatment) indicated that vehicle-treated retinas had 2.70% (+/-0.25% SD) cells were $CC3^+$, while TAKi-treated retinas contained 4.67% (+/-0.36% SD) (Figure 3.9H).

Inhibition of TAK1 leads to an increase in the number of pH3- and SOX2-labeled cells.

The localization of pTAK1 in dividing and differentiating cells led to the hypothesis that TAK1 was important in cell type-specific differentiation. If TAK1 was involved in cell cycle exit, the number of proliferating and/or retinal progenitor cells may increase in the presence of an inhibitor. To investigate whether there was a change in the number of dividing cells, retinas treated with vehicle or TAKi were sectioned and immunolabeled for pH3 (Ser10), a modification that is highly correlated with chromosomal condensation occurring in mitosis and meiosis [123]. Sections through the vehicle-treated retinas showed modest labeling for pH3 near the edge of the scleral edge of the retina (Figure 3.10A-C). In comparison, sections through TAKi-treated retinas showed a clear increase in the number of $pH3^+$ cells at the scleral edge, and it was apparent that some aberrantly labeled cells localized within to the GCL were also present (Figure 3.10D-F). Quantification of vehicle-treated retinas indicated 1.58% (+/- 0.19% SD) were $pH3^+$, while TAKi-treated contained 6.15% (+/- 0.52% SD) $pH3^+$ cells (Figure 3.10G).

Localization of retinal progenitor cells was carried out localizing and quantitating cells positive for progenitor marker SOX2 in vehicle and TAKi-treated ex-ovo retinas (Figure 3.10H-N). In vehicle-treated retinas, SOX2 was abundant in the elongated nuclei of retinal progenitors in the neuroblast layer as well as in dividing cells at the scleral edge (Figure 3.10I-K). SOX2 also labeled cells primarily in the neuroblast layer of the TAKI-treated retina; however, the number of labeled nuclei appeared much greater than the vehicle-treated retinas and the labeled nuclei are round in appearance rather than the normal elongated nuclei (Figure 3.10L-N). Quantitation of SOX2-labeled cells upheld the observation that there were more labeled cells in the TAKi-treated retinas (78.24% +/- 3.09%SD) in comparison to vehicle-treated retinas (54.10% +/-2.42% SD) (Figure 3.10H).

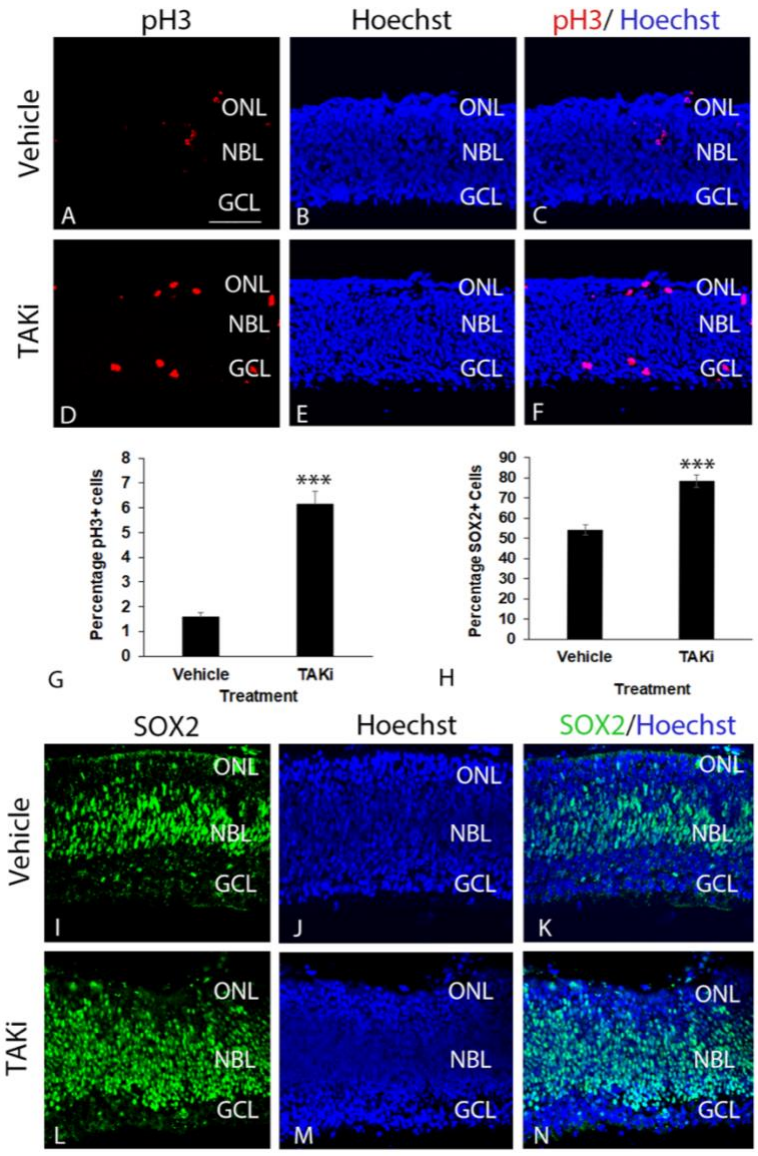

Figure 3.10 Taki-treated retinas have an increase in pH3+ and SOX2+ retinal progenitors in comparison to vehicle-treated retinas. E6 chick retinal cultures were treated with vehicle or 2μm TAK1 inhibitor (TAKi) for 24 hours and sections through retinas were co-labeled for cell division marker phospho-histone 3 (pH3; A, C, D, F) or progenitor marker SOX2 (I, K, L, N) and Hoechst dye for DNA (blue; B, C, E, F, J, K, M, N). Percentages of labeled cells were quantified in 3 separate retinas for pH3+ cells (G) or SOX2+ cells(H). Standard deviation is shown in G and H. A = 50μm for images A-F and I-N. Abbreviations: ONL, outer nuclear layer; NBL, neuroblast layer; GCL, ganglion cell layer. Scale bar in A = 50μm for images A-F and I-N.

Inhibition of TAK1 also leads to an increased number of cells labeled with visinin, islet1, NAPA73, and Brn3a.

To determine if there was a change in the number of cells expressing differentiation-specific markers, we treated ex-ovo retinal cultures with vehicle or TAKi, localized and quantitated cells expressing visinin, islet1, NAPA73, and BRN3A (Figure 3.11). The ex-ovo cultures could not be cultured for long periods of time, hence the analysis was focused primarily on retinal cells that differentiate early, such as cones (Visinin) and ganglion cells (NAPA73 and BRN3A). The number of Visinin+ cells in vehicle-treated retina averaged was 7.29 cells per section (+/- 0.82, N= 4 retinas), whereas TAKi-treated cells per section averaged 12.68 (+/-1.46, N=3 retinas). Likewise, immunolabel for NAPA in vehicle-treated retinas showed an average of 10.91 cells per section (+/- 1.43, N=4 retinas) and TAKi-treated samples showed an average of 21.80 cells per section (+/- 0.84, N=4). Brn3a+ cells showed a similar increase, with vehicle-treated retinas showing 3.15 cells per section (+/- .021, N=4) and TAKi-treated an average of 11.30 per section (+/-0.74, N=4). Islet1, a marker that has been shown to label cells undergoing differentiation, labels primarily ganglion cells at early stages, but later is found in most cells of the retina [124]. For this study, we used islet1 as a gauge of differentiation within the retina. Vehicle-treated retinas contained an average of 8.25 (+/-0.59, N=4 retinas) labeled cells per section. In comparison, TAKi-treated retinas contained an average of 15.92 (+/-0.23, N=4 retinas). With each marker, it was clear there were more differentiated cells within the TAKi-treated retinas in comparison to vehicle-treated retinas.

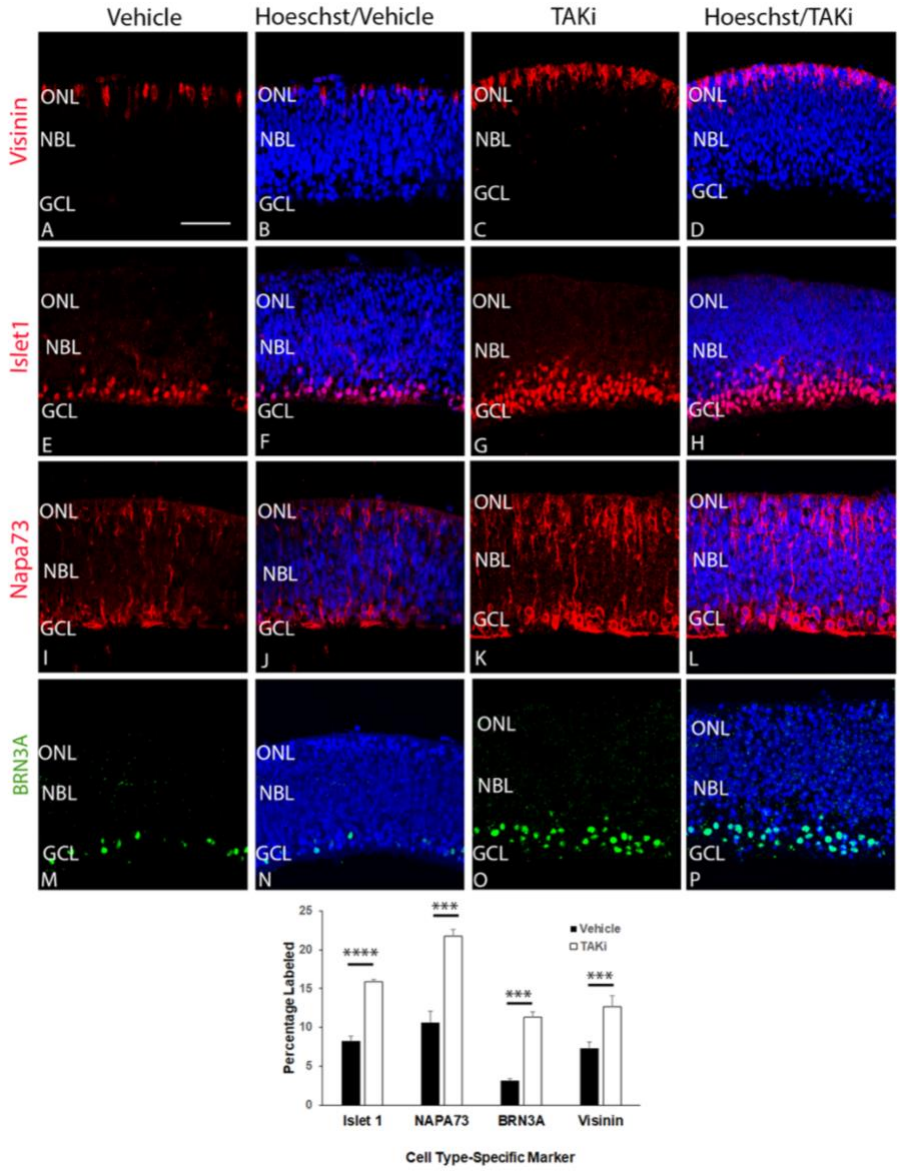

Figure 3.11 Sections through TAKi-treated retinas show an increased percentage of cells expressing cell type-specific markers Visinin, Islet1, NAPA73, and BRN3A in comparison to vehicle-treated retinas. E6 chick retinal cultures were treated with vehicle or 2mM TAK1 inhibitor (TAKi) for 24 hours and sections through retinas were co-labeled with Hoechst dye (DNA; blue) and visinin (A-D), islet1 (E-H), napa73 (I-L), or BRN3A (M-P). Abbreviations: NBL, neuroblast layer; GCL, ganglion cell layer. Scale bar in A = 50μm for images A-C.

3.5 DISCUSSION

The present study focused on the role of TAK1 in the developing chick retina. Immunolocalization of pTAK1 with markers present in progenitor and differentiating retinal cells

indicated that pTAK1 was widely expressed in progenitor (dividing and non-dividing) and differentiating cells of the retina, although expression in dividing progenitors and differentiating cell populations was heavier than expression noted in progenitors that were not actively dividing. *Ex vivo* E6 retinal cultures treated with TAK1 inhibitor, 5Z-7-oxozeaenol, for 24 hours showed an increase in 1) progenitor cells (both actively undergoing mitosis and those that were not actively dividing), 2) apoptotic cells, and 3) cones and ganglion cells.

TAK1 in Cell Cycle Regulation

Prior to conducting this study, we hypothesized that TAK1 played a role in differentiation, as has been suggested by studies in other tissues [1, 82, 113, 121]. However, results using TAK1 inhibition in conjunction with *ex-vivo* retinal cultures indicated there was an increase in cell type-specific differentiation, an increase in proliferating progenitors, and an increase (albeit small) in apoptosis. Together, these results suggest that TAK1 may not be limited to a role in differentiation but may play a broader role in cell cycle progression. Previous studies have shown that cell cycle length increases during neural development, brought about by an increase in the G1 phase of the cell cycle [125, 126]. More recent studies in murine central nervous system have shown that there may also be a lengthening of the S phase in progenitors during development [95]. A lengthening in the G1 phase of the cell cycle is associated with a decrease in proliferation and an increase in cells leaving the cell cycle to differentiate [126-128]. Cyclin D is essential for the progression of proliferating cells from G1 to S phase, such that an overexpression of cyclin D decreases the length of G1 phase and knockdown of cyclin D increases the length of G1 substantially [129]. Moreover, overexpression of cyclin A2, normally important in both S and G2 phases, shortens cell cycle length in Xenopus, reducing neuronal differentiation [130]. TAK1 also has some revealing links to the cell cycle.

TAK1 has been shown to directly affect levels of both cyclins D1 and A, although none have been shown in the central nervous system [131, 132]. A constitutively active form of TAK1 expressed in kidney cells reduces ^{3}H uptake by cells as well as passage through G2 to M phases. Further investigation indicated the constitutively active form of TAK1 inhibited both cyclin D1 and cyclin A promoter activity and the expression of protein [131]. Cyclin D1 is critical for progression of cells through the G1 phase of the cell cycle, while cyclin A is important in both synthesis and

mitosis [131, 133]. This finding is indicative of TAK1 inhibiting progression though G1 of the cell cycle, consistent with our observations that the inhibition of TAK1 in the retina leads to an increase in cell cycle progression and an increase in synthesis and G2 to M transition, leading to an increase in both proliferating and differentiating cells. TAK1 has also been implicated in reducing cell cycle progression following DNA damage in cells [134]. Inactive tousled-like kinase (TLK) bound to TAK1 increased p38 kinase activity, leading to an increased G2 phase. Collectively, these studies suggest that TAK1 is playing a key role in cell cycle progression, which is also indicated by our findings.

In our working model (Figure 3.12), we propose a physiological role for TAK1 in developing retina in cell cycle progression.

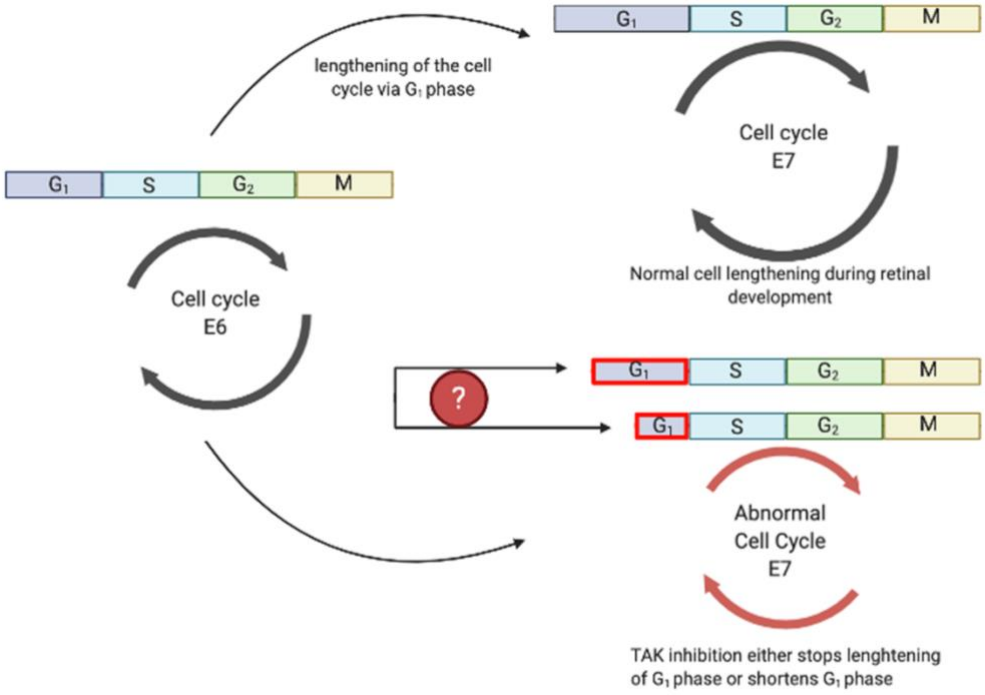

Figure 3.12 Proposed model of TAK1 action in normal cell cycle progression, the G1 phase lengthens in successive generation of progenitors. Cells with lengthened G1 phase will eventually enter G0 and differentiate (upper diagram). In the presence of TAK1 inhibitor, the G1 phase does not lengthen in a subpopulation of cells. Progenitor cells with a cell cycle that has not lengthened will continue proliferating.

During normal development, TAK1 may reduce the activity of cyclin D1, allowing the cycle to lengthen in G1, and increasing the number of cells that leave the cell cycle. When TAK1 activity is decreased, there is less disruption to cyclin D1 activity, allowing cells to progress through G1 and the rest of the cell cycle, leading to an increase in cells that proliferate. By increasing cells that proliferate, it ensures an increase in cells that can also escape the cell cycle and differentiate. However, according to Lange and Huttner [129], the "cell cycle length hypothesis" states that the length of G1 phase determines differentiation and that G1 functions in terms of a threshold; when G1 is below a certain threshold, differentiation does not occur. G1 phase beyond this threshold is what is necessary to drive differentiation, along with bHLH [126]. Transcription factors of the bHLH proneural family are considered the master regulators of neurogenesis and are responsible for controlling progenitor maintenance through the Notch-Delta pathway, cell cycle exit, and differentiation [126]. If the cell cycle length hypothesis holds true and G1 exhibits a threshold, this could possibly explain why our results show both an increase in proliferation and differentiation. Future studies will focus on investigating the link between TAK1, cell cycle progression, and the threshold in G1 phase of the cell cycle.

TAK1 in Apoptosis

TAK1 has been implicated in survival, apoptosis and necroptosis, depending on extracellular and intracellular context [1, 135]. Survival appears to involve transcription of genes downstream of nuclear factor kappa-light-chain-enhancer of activated B (NFκB) and c-jun-N-terminal kinase (JNK). Studies using a dominant negative form of TAK1 in liver have shown that quiescent cells re-enter the cell cycle via expression of c-Myc [136]. While c-Myc can drive cells into division it has also been shown to induce apoptosis. Cell death induced by c-Myc has been shown to be connected to the activation of apoptotic factors caspase-3 and c-Jun N-terminal kinases (JNKs) [137]. Whether the activation of NFkB leads to survival, apoptosis, or necroptosis is likely to depend on various present factors. RIPK1 and RIPK3 factors lead to necroptosis, JNK apoptosis, ATG5 and Beclin1 in autophagy [135].

Multiple studies have shown that c-Myc is necessary for apoptosis in response to pathologies such as cancers, DNA damage, and chemotoxins [138]. In the central nervous system, a study found that in microglia, activated TAK1 resulted in an increase in pro-inflammatory cytokines and

apoptosis [61]. TAK1 inhibition in cancer cells *in vitro* has shown an increase in apoptosis through the inhibition of TNF survival and inflammatory signaling [139]. TAK1 has also been found to regulate cell survival through oxidative stress and receptor-interacting protein kinase 1 (RIPK1) and when TAK1 is inhibited or knocked out, it results in apoptosis in most tissue types [1]. TAK1 inhibition or dysregulation results in abnormalities that could be key to learning more about human pathologies.

TAK1 in Maintenance of the Retina and in Pathology

In these studies, we have shown that TAK1 is more widespread within cell types of the retina than previously observed. Collectively, the results of this study lead to the suggestion that TAK1 is responsible for increased cell cycle length within the developing chick retina. Previous work has shown that TAK1 expression that is found in the chick retina is similar to the TAK1 expression found in the human retina [60]. Activated TAK1 has been found to be present in all layers of a normal retina while it is barely detectable in pathological retinas [60]. This similarity between TAK1 prevalence in chick and human retinas sheds light on possible approaches for studying human retinal pathologies. TAK1 has been implicated and shown to be involved in cell proliferation, cell death, and most importantly, cell cycle progression. Future studies exploring TAK1s role in the cell cycle, proliferation, and cell death could elucidate potential therapies for retinal abnormalities and diseases.

REFERENCES

1. Mihaly, S.R., J. Ninomiya-Tsuji, and S. Morioka, *TAK1 control of cell death.* Cell Death Differ, 2014. **21**(11): p. 1667-76

2. Ajibade, A.A., H.Y. Wang, and R.F. Wang, *Cell type-specific function of TAK1 in innate immune signaling.* Trends Immunol, 2013. **34**(7): p. 307-16.

3. Bosman, M.C., et al., *The TAK1-NF-kappaB axis as therapeutic target for AML.* Blood, 2014. **124**(20): p. 3130-40.

4. Goldmann, T., et al., *A new type of microglia gene targeting shows TAK1 to be pivotal in CNS autoimmune inflammation.* Nat Neurosci, 2013. **16**(11): p. 1618-26.

5. Lachke, S.A. and R.L. Maas, *Building the developmental oculome: systems biology in vertebrate eye development and disease.* Wiley Interdiscip Rev Syst Biol Med, 2010. **2**(3): p. 305-323.

6. Stenkamp, D.L., *Development of the Vertebrate Eye and Retina.* Prog Mol Biol Transl Sci, 2015. **134**: p. 397-414.

7. L. Chow, R., *Early Eye Development In Vertebrates.* Cell Dev. Biol. , 2001(17): p. 255-296.

8. Webvision. *The Organization of the Retina and Visual System* [Online Book] 2012 [cited 2012; Available from: http://webvision.med.utah.edu/

9. Wu, J., et al., *Mechanism and in vitro pharmacology of TAK1 inhibition by (5Z)-7-Oxozeaenol.* ACS Chem Biol, 2013. **8**(3): p. 643-50.

10. Yang, X.J., *Roles of cell-extrinsic growth factors in vertebrate eye pattern formation and retinogenesis.* Semin Cell Dev Biol, 2004. **15**(1): p. 91-103.

11. Cantrup, R.T., *The role of the tumor suppressor gene 'Pten' during retinal development.* 2012.

12. Gilbert, C.D. and W. Li, *Top-down influences on visual processing.* Nat Rev Neurosci, 2013. **14**(5): p. 350-63.

13. Masland, R.H., *Cell populations of the retina: the Proctor lecture.* Invest Ophthalmol Vis Sci, 2011. **52**(7): p. 4581-91.

14. Care, I.f.Q.a.E.i.H. *How does the eye work?* [Website] 2009 2018; Available from: https://www.ncbi.nlm.nih.gov/books/NBK279248/.

15. Yan, R.-T., et al., *bHLH Genes and Retinal Cell Fate Specification.* Mol Neurobiol, 2005.

16. Dennis, D.J., S. Han, and C. Schuurmans, *bHLH transcription factors in neural development, disease, and reprogramming.* Brain Res, 2019. **1705**: p. 48-65.

17. Wassle, H., et al., *Glycinergic transmission in the Mammalian retina.* Front Mol Neurosci, 2009. **2**: p. 6.

18. Franze, K., et al., *Muller cells are living optical fibers in the vertebrate retina.* Proc Natl Acad Sci U S A, 2007. **104**(20): p. 8287-92.

19. Cebulla, C.M., et al., *A chick model of retinal detachment: cone rich and novel.* PLoS One, 2012. **7**(9): p. e44257.

20. Bringmann, A., et al., *GABA and Glutamate Uptake and Metabolism in Retinal Glial (Muller) Cells.* Front Endocrinol (Lausanne), 2013. **4**: p. 48.

21. Koeppen, B. and B. Stanton, *Berne & Levy Physiology*. 2017, Elsevier. p. 880.

22. Hollander, H., et al., *Structure of the macroglia of the retina: sharing and division of labour between astrocytes and Muller cells.* J Comp Neurol, 1991. **313**(4): p. 587-603.

23. Lenkowski, J.R. and P.A. Raymond, *Muller glia: Stem cells for generation and regeneration of retinal neurons in teleost fish.* Prog Retin Eye Res, 2014. **40**: p. 94-123.

24. Vecino, E., et al., *Glia-neuron interactions in the mammalian retina.* Prog Retin Eye Res, 2016. **51**: p. 1-40.

25. Dyer, M.A., & Cepko, C. L., *Control of Muller glial cell proliferation and activation following retinal injury.* Nature America, 2000. **3**(9).

26. O'Sullivan, M.L., et al., *Astrocytes follow ganglion cell axons to establish an angiogenic template during retinal development.* Glia, 2017. **65**(10): p. 1697-1716.

27. Ginhoux, F. and M. Prinz, *Origin of microglia: current concepts and past controversies.* Cold Spring Harb Perspect Biol, 2015. **7**(8): p. a020537.

28. Kierdorf, K. and M. Prinz, *Factors regulating microglia activation.* Front Cell Neurosci, 2013. **7**: p. 44.

29. Olson, J.K. and S.D. Miller, *Microglia initiate central nervous system innate and adaptive immune responses through multiple TLRs.* J Immunol, 2004. **173**(6): p. 3916-24.

30. Silverman, S.M. and W.T. Wong, *Microglia in the Retina: Roles in Development, Maturity, and Disease.* Annu. Rev. Vis. Sci., 2018.

31. Paolicelli, R.C., et al., *Synaptic Pruning by Microglia Is Necessary for Normal Brain Development*. 2011: Science.

32. Arnold, T. and C. Betsholtz, *The importance of microglia in the development of the vasculature in the central nervous system.* Vascular Cell, 2013. **5**.

33. Kinuthia, U.M., A. Wolf, and T. Langmann, *Microglia and Inflammatory Responses in Diabetic Retinopathy.* Front Immunol, 2020. **11**: p. 564077.

34. Selvam, S., T. Kumar, and M. Fruttiger, *Retinal vasculature development in health and disease.* Prog Retin Eye Res, 2018. **63**: p. 1-19.

35. Fu, Z., et al., *Targeting Neurovascular Interaction in Retinal Disorders.* Int J Mol Sci, 2020. **21**(4).

36. Runkle, E.A., *Methods in Molecular Biology*. The Blood-Brain and Other Neural Barriers, ed. S. Nag. 2011: Springer Protocols.

37. Trost, A., et al., *Brain and Retinal Pericytes: Origin, Function and Role.* Front Cell Neurosci, 2016. **10**: p. 20.

38. Hellström, M., et al., *Role of PDGF-B and PDGFR-B in recruitment of vascular smooth muscle cells and pericytes during embryonic blood vessel formation in the mouse.* Development, 1999. **126**.

39. Geevarghese, A. and I.M. Herman, *Pericyte-endothelial crosstalk: implications and opportunities for advanced cellular therapies.* Transl Res, 2014. **163**(4): p. 296-306.

40. Hellström, M., et al., *Lack of Pericytes Leads to Endothelial Hyperplasia and Abnormal Vascular Morphogenesis.* The Journal of Cell Biology, 2001. **153**: p. 543-553.

41. Rudraraju, M., S.P. Narayanan, and P.R.d.j.p. Somanath, *Regulation of blood-retinal barrier cell-junctions in diabetic retinopathy.* Pharmacological Research, 2020.

42. Harrell, C.R., B. Simovic Markovic, and C. Fellabaum, *Molecular mechanisms underlying therapeutic potential of pericytes.* J Biomed Sci 2018. **25**.

43. Salsani, A. and M. Nathan, *A Review of Types 2 and 2 Diabetes Mellitus and Their Treatment with Insulin.* American Journal of Therapeutics, 2006. **13**: p. 349-361.

44. Prevention, C.f.D.C.a., *National Diabetes Statistics Report, 2020*. 2020, U.S. Dept of Health and Human Services: Atlanta, GA.

45. Saadine, B.J., D. Fong, and J. Yao, *Factors Associated with Follow-up Eye Examination Among Persons with Diabetes.* Ophthalmic Communications Society, 2008.

46. Wang, W. and A.C.Y. Lo, *Diabetic Retinopathy: Pathophysiology and Treatments.* Int J Mol Sci, 2018. **19**(6).

47. Viswanath, K.M.D.M. and M.D.D. McGavin, *Diabetic Retinopathy: Clinical Findings and Maangement.* Community Eye Health 2003. **16**.

48. Hammer, S.S., et al., *The Mechanism of Diabetic Retinopathy Pathogenesis Unifying Key Lipid Regulators, Sirtuin 1 and Liver X Receptor.* EBioMedicine, 2017. **22**: p. 181-190.

49. Frank, R.N.M., *Diabetic Retinopathy.* The New England Journal of Medicine, 2004. **350**: p. 48-58.

50. *Diabetes & Eye Exams*. Available from: http://cceyemd.com/diabetes-eye-exams/.

51. Burotto, M., et al., *The MAPK pathway across different malignancies: a new perspective.* Cancer, 2014. **120**(22): p. 3446-56.

52. Sweeney, M.D., S. Ayyadurai, and B.V. Zlokovic, *Pericytes of the neurovascular unit: key functions and signaling pathways.* Nat Neurosci, 2016. **19**(6): p. 771-83.

53. Donovan, M., F. Doonan, and T.G. Cotter, *Differential roles of ERK1/2 and JNK in retinal development and degeneration.* J Neurochem, 2011. **116**(1): p. 33-42.

54. Du, Y., et al., *Effects of p38 MAPK inhibition on early stages of diabetic retinopathy and sensory nerve function.* Invest Ophthalmol Vis Sci, 2010. **51**(4): p. 2158-64.

55. Hirata, K. and K. Kubo, *Relationship between Blood Levels of N-Carboxymethyl-lysine and Pentosidine and the Severity of Microangiopathy in Type 2 Diabetes.* Endocrine Journal, 2004. **51**: p. 537-544.

56. Morioka, S., et al., *TAK1 kinase signaling regulates embryonic angiogenesis by modulating endothelial cell survival and migration.* Blood, 2012. **120**(18): p. 3846-57.

57. Romeo, G., et al., *Activation of Nuclear Factor- kB Induced by Diabetes and High Glucose Regulates a Proapoptotic Program in Retinal Pericytes.* Diabetes, 2002. **51**.

58. Scarneo, S.A., et al., *Genetic and pharmacological validation of TAK1 inhibition in macrophages as a therapeutic strategy to effectively inhibit TNF secretion.* Sci Rep, 2018. **8**(1): p. 17058.

59. Tang, M., et al., *TAK1 is required for the survival of hematopoietic cells and hepatocytes in mice.* J Exp Med, 2008. **205**(7): p. 1611-9.

60. Dvashi, Z., et al., *Aberrant Activity of TAK1 is Associated with Retinal Pathology.* Journal of Cytology & Histology, 2016.

61. Zeyen, T., et al., *Microglial-specific depletion of TAK1 is neuroprotective in the acute phase after ischemic stroke.* J Mol Med (Berl), 2020. **98**(6): p. 833-847.

62. Cheung, N., P. Mitchell, and T.Y. Wong, *Diabetic retinopathy.* The Lancet, 2010. **376**(9735): p. 124-136.

63. Xu, H. and M. Chen, *Diabetic retinopathy and dysregulated innate immunity.* Vision Res, 2017. **139**: p. 39-46.

64. Hammes, H.P., et al., *Pericytes and the Pathogenesis of Diabetic Retinopathy.* Diabetes, 2002. **51**.

65. Netto, J.P., et al., *Neurovascular Unit: Basic and Clinical Imaging with Emphasis on Advantages of Ferumoxytol.* Neurosurgery, 2018. **82**(6): p. 770-780.

66. Creager, M.A., et al., *Diabetes and vascular disease: pathophysiology, clinical consequences, and medical therapy: Part I.* Circulation, 2003. **108**(12): p. 1527-32.

67. Sofroniew, M.V., *Astrocyte barriers to neurotoxic inflammation.* Nat Rev Neurosci, 2015. **16**(5): p. 249-63.

68. Chibber, R., et al., *Toxic action of advanced glycation end products on cultured retinal capillary pericytes and endothelial cells: relevance to diabetic retinopathy.* Diabetologia, 1997. **40**: p. 156-164.

69. Kern, T.S., J. Tang, and B.A. Berkowitz, *Validation of structural and functional lesions of diabetic retinopathy in mice.* Molecular Vision, 2010. **16**: p. 2121-2131.

70. Tang, J. and T.S. Kern, *Inflammation in diabetic retinopathy.* Prog Retin Eye Res, 2011. **30**(5): p. 343-58.

71. Ferland-McCollough, D., et al., *Pericytes, an overlooked player in vascular pathobiology.* Pharmacol Ther, 2017. **171**: p. 30-42.

72. Kowluru, R.A. and P.S. Chan, *Oxidative stress and diabetic retinopathy.* Exp Diabetes Res, 2007. **2007**: p. 43603.

73. Shin, E.S., C.M. Sorenson, and N. Sheibani, *Diabetes and retinal vascular dysfunction.* J Ophthalmic Vis Res, 2014. **9**(3): p. 362-73.

74. Yuan, T., et al., *New insights into oxidative stress and inflammation during diabetes mellitus-accelerated atherosclerosis.* Redox Biol, 2019. **20**: p. 247-260.

75. Geraldes, P., et al., *Activation of PKC-delta and SHP-1 by hyperglycemia causes vascular cell apoptosis and diabetic retinopathy.* Nat Med, 2009. **15**(11): p. 1298-306.

76. Wang, S., *INFLAMMATION IN THE EARLY PATHOGENESIS OF DIABETIC RETINOPATHY*, in *Biology*. 2018, Purdue University

77. Liu, T., et al., *NF-kappaB signaling in inflammation.* Signal Transduct Target Ther, 2017. **2**.

78. Livolsi, A., et al., *Tyrosine phosphorylation-dependent activation of NFκB Requirement for p56 LCK and ZAP-70 protein tyrosine kinases.* Eur. J. Biochem, 2001. **268**: p. 1508-1515.

79. Roque, R.S. and R.B. Caldwell, *Isolation and culture of retinal microglia.* Current Eye Research, 1993.

80. Kim, B., et al., *Sex differences in glucose metabolism of streptozotocin-induced diabetes inbred mice (C57BL/6J).* Applied Biological Chemistry, 2020. **63**(1).

81. Mostafavinia, A., et al., *The effects of dosage and the routes of administrations of streptozotocin and alloxan on induction rate of type1 diabetes mellitus and mortality rate in rats.* Lab Anim Res, 2016. **32**(3): p. 160-165.

82. Blonska, M., et al., *TAK1 is recruited to the tumor necrosis factor-alpha (TNF-alpha) receptor 1 complex in a receptor-interacting protein (RIP)-dependent manner and cooperates with MEKK3 leading to NF-kappaB activation.* J Biol Chem, 2005. **280**(52): p. 43056-63.

83. Lee, J., L. Mira-Arbibe, and R. Ulevitch, J., *TAK1 regulates multiple protein kinase cascades activated by bacterial lipopolysaccharide.* Journal of Leukocyte Biology, 2000. **68**.

84. Hayden, M.S. and S. Ghosh, *Regulation of NF-kappaB by TNF family cytokines.* Semin Immunol, 2014. **26**(3): p. 253-66.

85. Irie, T., T. Muta, and K. Takeshige, *TAK1 mediates an activation signal from toll-like receptor(s) to nuclear factor-kB in lipopolysaccharide-stimulated macrophages.* FEBS Letters, 1999. **467**: p. 160-164.

86. Lin, Y., S. Jamison, and W. Lin, *Interferon-gamma activates nuclear factor-kappa B in oligodendrocytes through a process mediated by the unfolded protein response.* PLoS One, 2012. **7**(5): p. e36408.

87. Clark, M., C.J. Kroger, and R.M. Tisch, *Type 1 Diabetes: A Chronic Anti-Self-Inflammatory Response.* Front Immunol, 2017. **8**: p. 1898.

88. Tsalamandris, S., et al., *The Role of Inflammation in Diabetes: Current Concepts and Future Perspectives.* Eur Cardiol, 2019. **14**(1): p. 50-59.

89. Aluganti Narasimhulu, C. and D.K. Singla, *The Role of Bone Morphogenetic Protein 7 (BMP-7) in Inflammation in Heart Diseases.* Cells, 2020. **9**(2).

90. Wang, J.S., et al., *TAK1 inhibition-induced RIP1-dependent apoptosis in murine macrophages relies on constitutive TNF-alpha signaling and ROS production.* J Biomed Sci, 2015. **22**: p. 76.

91. Turner, D.L., & Cepko, C. L. , *A common progenitor for neurons and glia persists in rat retina late in development.* Nature, 1987. **328**(6126): p. 131-136.

92. Holt, C.E., Bertsch, T. W., Ellis, H. M., & Harris, W. A., *Cellular determination in the xenopus retina is independent of lineage and birth date.* Neuron, 1988. **1**: p. 15-26.

93. Wetts, R., & Fraser, S. , *Multipotent precursors can give rise to all major cell types of the frog retina.* Science, 1988. **239**(4844): p. 1142-1145.

94. Turner, D.L., Snyder, E. Y., & Cepko, C. L. , *Lineage-independent determination of cell type in the embryonic mouse retina.* Neuron, 1990. **4**(6): p. 833-845.

95. Arai, Y., et al., *Neural stem and progenitor cells shorten S-phase on commitment to neuron production.* Nat Commun, 2011. **2**: p. 154.

96. Ferree, P.L., V.E. Deneke, and S. Di Talia, *Measuring time during early embryonic development.* Semin Cell Dev Biol, 2016. **55**: p. 80-8.

97. Cepko, C.L., *The roles of intrinsic and extrinsic cues and bHLH genes in the determination of retinal cell fates.* Current Opinion in Neurobiology, 1999. **9**(1): p. 37-46.

98. Jensen, A.M., & Raff, M. C., *Continuous Observation of Multipotential Retinal Progenitor Cells in Clonal Density Culture.* Developmental Biology, 1997. **188**(2).

99. Tomita, K., Ishibashi, M., Nakahara, K., Ang, S.-L., Nakanishi, S., Guillemot, F., & Kageyama, R. , *Mammalian hairy and Enhancer of Split Homolog 1 Regulates Differentiation of Retinal Neurons and Is Essential for Eye Morphogenesis.* Neuron, 1996. **16**: p. 723-734.

100. Ohnuma, S., Philpott, A., Wang, K., Holt, C. E., & Harris, W. A. , *p27Xic1, a Cdk Inhibitor, Promotes the Determination of Glial Cells in Xenopus Retina.* Cell, 1992. **99**: p. 499-510.

101. Hatakeyama, J. and R. Kageyama, *Retinal cell fate determination and bHLH factors.* Semin Cell Dev Biol, 2004. **15**(1): p. 83-9.

102. Miles, A. and V. Tropepe, *Coordinating progenitor cell cycle exit and differentiation in the developing vertebrate retina.* Neurogenesis (Austin), 2016. **3**(1): p. e1161697.

103. Dyer, M.A., & Cepko, C. L. , *Regulating proliferation during retinal development.* Nature, 2001. **2**(5): p. 333-342.

104. Wagner, I., et al., *Serum Proteases Potentiate BMP-Induced Cell Cycle Re-entry of Dedifferentiating Muscle Cells during Newt Limb Regeneration.* Dev Cell, 2017. **40**(6): p. 608-617 e6.

105. Vogel, T., et al., *Transforming growth factor beta promotes neuronal cell fate of mouse cortical and hippocampal progenitors in vitro and in vivo: identification of Nedd9 as an essential signaling component.* Cereb Cortex, 2010. **20**(3): p. 661-71.

106. Roy, S. and P.W. Ingham, *Hedgehogs tryst with the cell cycle.* J Cell Sci, 2002. **115**(Pt 23): p. 4393-7.

107. Jarrin, M., T. Pandit, and L. Gunhaga, *A balance of FGF and BMP signals regulates cell cycle exit and Equarin expression in lens cells.* Mol Biol Cell, 2012. **23**(16): p. 3266-74.

108. Hunter, T., *Braking the Cycle.* Cell, 1993. **75**(5): p. 839-841.

109. Edgar, B., *Diversification of cell cycle controls in developing embryos.* Current Opinion in Cell Biology, 1995. **7**(6): p. 815-824.

110. Shkumatava, A. and C.J. Neumann, *Shh directs cell-cycle exit by activating p57Kip2 in the zebrafish retina.* EMBO Rep, 2005. **6**(6): p. 563-9.

111. Friedrichs, M., Wirsdöerfer, F., Flohé, S. B., Schneider, S., Wuelling, M., & Vortkamp, A. , *BMP signaling balances proliferation and differentiation of muscle satellite cell descendants.* Cell Biology, 2011. **12**(26).

112. Zhang, P., Wong, C., DePinho, R. A., Harper, J. W., & Elledge, S. J. , *Cooperation between the Cdk inhibitors p27KIP1 and p57KIP2 in the control of tissue growth and development.* Genes & Development, 1998. **12**(20): p. 3162-3167.

113. Ninomiya-Tsuji, J., Kishimoto, K., Hiyama, A., Inoue, J., Cao, Z., & Matsumoto, K. , *The kinase TAK1 can activate the NIK-IκB as well as the MAP kinase cascade in the IL-1 signalling pathway.* Nature, 1999. **298**(6724): p. 252-256.

114. Sato, S., et al., *Essential function for the kinase TAK1 in innate and adaptive immune responses.* Nat Immunol, 2005. **6**(11): p. 1087-95.

115. Munoz-Sanjuan, I., et al., *Gene profiling during neural induction in Xenopus laevis: regulation of BMP signaling by post-transcriptional mechanisms and TAB3, a novel TAK1-binding protein.* Development, 2002. **129**(23): p. 5529-40.

116. Choi, M.E., Y. Ding, and S.I. Kim, *TGF-beta signaling via TAK1 pathway: role in kidney fibrosis.* Semin Nephrol, 2012. **32**(3): p. 244-52.

117. Hong, S., et al., *Agmatine protects retinal ganglion cells from hypoxia-induced apoptosis in transformed rat retinal ganglion cell line.* BMC Neurosci, 2007. **8**: p. 81.

118. Syc-Mazurek, S.B., et al., *Mkk4 and Mkk7 are important for retinal development and axonal injury-induced retinal ganglion cell death.* Cell Death Dis, 2018. **9**(11): p. 1095.

119. Shirazi Fard, S., M. Blixt, and F. Hallbook, *Whole Retinal Explants from Chicken Embryos for Electroporation and Chemical Reagent Treatments.* J Vis Exp, 2015(103).

120. Morrow, E.M., Belliveau, M. J., & Cepko, C. L. , *Two Phases of Rod Photoreceptor Differentiation during Rat Retinal Development.* The Journal of Neuroscience, 1998. **18**(10): p. 3738-3748.

121. Lamothe, B., et al., *TAK1 is essential for osteoclast differentiation and is an important modulator of cell death by apoptosis and necroptosis.* Mol Cell Biol, 2013. **33**(3): p. 582-95.

122. Shin, J.H., et al., *TAK1 regulates autophagic cell death by suppressing the phosphorylation of p70 S6 kinase 1.* Sci Rep, 2013. **3**: p. 1561.

123. Van Hooser A, G.D., Allis CD, Brinkley BR, Mancini MA., *Histone H3 phosphorylation is required for the initiation, but not maintenance, of mammalian chromosome condensation.* J Cell Sci., 1998. **111**: p. 3497-3506.

124. Gutierrez, C., McNally, M. & Canto-Soler, M.V., *Cytoskeleton proteins previously considered exclusive to Ganglion Cells are transiently expressed by all retinal neuronal precursors.* BMC Dev Biol, 2011. **11**(46).

125. Ohnuma, S., Harris, W. A., *Neurogenesis and the Cell Cycle.* Neuron, 2003. **40**: p. 199-208.

126. Hardwick, L.J., et al., *Cell cycle regulation of proliferation versus differentiation in the central nervous system.* Cell Tissue Res, 2015. **359**(1): p. 187-200.

127. Lange, C. and F. Calegari, *Cdks and cyclins link G1 length and differentiation of embryonic, neural and hematopoietic stem cells.* Cell Cycle, 2010. **9**(10): p. 1893-900.

128. Calegari, F., et al., *Selective lengthening of the cell cycle in the neurogenic subpopulation of neural progenitor cells during mouse brain development.* J Neurosci, 2005. **25**(28): p. 6533-8.

129. Lange, C., W.B. Huttner, and F. Calegari, *Cdk4/cyclinD1 overexpression in neural stem cells shortens G1, delays neurogenesis, and promotes the generation and expansion of basal progenitors.* Cell Stem Cell, 2009. **5**(3): p. 320-31.

130. Richard-Parpaillon, L., et al., *G1/S phase cyclin-dependent kinase overexpression perturbs early development and delays tissue-specific differentiation in Xenopus.* Development, 2004. **131**(11): p. 2577-86.

131. Terada, Y., et al., *TGF-beta-activating kinase-1 inhibits cell cycle and expression of cyclin D1 and A in LLC-PK1 cells.* Kidney Int, 1999. **56**(4): p. 1378-90.

132. Terada, Y., et al., *Regulation of cyclin D1 expression and cell cycle progression by mitogen-activated protein kinase cascade.* Kidney Int, 1999. **56**(4): p. 1258-61.

133. Michele Pagano1, R.P., W.A.a. Fulvia Verde3, and G. Draetta', *Cyclin A is required at two points in the human cell cycle.* EMBO Rep, 1992. **11**: p. 961-971.

134. Liaw, G.J. and C.S. Chiang, *Inactive Tlk associating with Tak1 increases p38 MAPK activity to prolong the G2 phase.* Sci Rep, 2019. **9**(1): p. 1885.

135. Verzella, D., et al., *Life, death, and autophagy in cancer: NF-kappaB turns up everywhere.* Cell Death Dis, 2020. **11**(3): p. 210.

136. Schnabl, B., et al., *TAK1/JNK and p38 have opposite effects on rat hepatic stellate cells.* Hepatology, 2001. **34**(5): p. 953-63.

137. Dhanasekaran, D.N. and E.P. Reddy, *JNK signaling in apoptosis.* Oncogene, 2008. **27**(48): p. 6245-51.

138. Prendergast, G.C., *Mechanisms of apoptosis by c-Myc.* Oncogene, 1999. **18**.

139. Scarneo, S., et al., *TAK1 regulates the tumor microenvironment through inflammatory, angiogenetic and apoptotic signaling cascades.* Oncotarget, 2020. **11**: p. 1961-1970.